An Underground Mine Ore Pass System Optimization via Fuzzy 0–1 Linear Programming with Novel Torricelli–Simpson Ranking Function

Dževdet Halilović, Miloš Gligorić, Zoran Gligorić, Dragan Pamučar

mathematics

MDPI

Article

An Underground Mine Ore Pass System Optimization via Fuzzy 0–1 Linear Programming with Novel Torricelli–Simpson Ranking Function

Dževdet Halilović [1], Miloš Gligorić [1,*], Zoran Gligorić [1] and Dragan Pamučar [2,3]

[1] Faculty of Mining and Geology, University of Belgrade, Đušina 7, 11000 Belgrade, Serbia; dzevdet.halilovic@rgf.bg.ac.rs (D.H.); zoran.gligoric@rgf.bg.ac.rs (Z.G.)
[2] Department of Operations Research and Statistic, Faculty of Organizational Sciences, University of Belgrade, Jove Ilića 154, 11000 Belgrade, Serbia; dragan.pamucar@fon.bg.ac.rs
[3] College of Engineering, Yuan Ze University, No. 135, Yuandong Rd, Zhongli District, Taoyuan City 320, Taiwan
* Correspondence: milos.gligoric@rgf.bg.ac.rs

Abstract: In this work, we propose a 3D dynamic optimization model that enables the design of an underground mine ore pass system with uncertainties. Ore transportation costs and ore pass development costs are quantified by triangular fuzzy numbers. Transportation costs are treated as production costs, and they vary over the duration of mining operation, while development costs of ore passes are treated as an investment, and they are treated as constant. The developed model belongs to the class of fuzzy 0–1 linear programming models, where the fuzzy objective cost function achieves a minimum value, with respect to given set of techno-dynamic constraints. Searching for optimal value in the fuzzy environment is a hard task, and because of that, we developed a new ranking function which transforms the fuzzy optimization model into a crisp one. A triangular fuzzy number can be presented as a triangular graph G(V,E) composed of vertices and edges. The x-coordinate of the Torricelli point of a triangular graph presents the crisp value of a triangular fuzzy number. The use of this model lets us know the optimal number of ore passes, optimal location of ore passes, and optimal dynamic ore transportation plan.

Keywords: ore pass; optimization; fuzzy linear programming; triangular graph; Torricelli point; ranking function

MSC: 90C90

Citation: Halilović, D.; Gligorić, M.; Gligorić, Z.; Pamučar, D. An Underground Mine Ore Pass System Optimization via Fuzzy 0–1 Linear Programming with Novel Torricelli–Simpson Ranking Function. *Mathematics* **2023**, *11*, 2914. https://doi.org/10.3390/math11132914

Academic Editors: Manuel Ivan Rodriguez Borbon and Hansuk Sohn

Received: 1 June 2023
Revised: 20 June 2023
Accepted: 23 June 2023
Published: 29 June 2023

1. Introduction

An ore pass is a vertical or near-vertical opening through which ore falls under gravity from upper levels to the lowest haulage level. In most cases, an ore pass system is associated with sublevel mining methods. It arises from the fact that a sublevel mining method is used when the dip of the ore deposit is steep (greater than about 55 degrees). A consistent issue in the optimization of ore pass system is the regulation of the total number of ore passes which connect a defined number of sublevels and the definition of ore pass locations as well. The aim of this paper is to understand challenges associated with such complex combinatorial problems and provide a tool for solving them. Generally, the ore passes optimization problem belongs to the class of location–allocation problems. In nature, the ore passes optimization problem is a 3D problem, because sublevels lie on distinct parallel planes. The dynamic nature of the problem comes from the dynamic plan of mining, while uncertainty is associated with the fluctuation in ore transportation costs and the costs of ore pass development.

Many authors have investigated the ore pass system in the context of its dimension, stability, shape or other structural design parameter. Maree [1] analyzed the possibility of

developing five new ore pass systems which would improve the existed haulage system and fulfill the planned production capacity. Also, Maree identified several critical design parameters that influence on optimal ore pass system creation and recommended some solutions to achieve the best practice function of an ore pass system. Hadjigeorgiou and Stacey [2] proposed six design principles during the ore pass design process to avoid stability problems and failures of an ore pass. They suggested the creation of a strategic plan that includes numerous tactical operations and actions to prevent ore pass collapses in order to provide ore pass longevity. Skawina et al. [3] studied the interrelationship and interdependence between ore passes, equipment for LHD operations and production rates. Fifteen scenarios for each of the three production areas have been simulated considering different number of ore passes and LHD machines where the effect of the ore pass loss on the LHD operations, such as production rate, is analyzed. Sredniawa et al. [4] presented a process for the renovation of ore passes based on various factors that influence ore pass longevity in Kiirunavaara Mine, in Sweden. Two production areas with a total of eight ore passes have been analyzed, and the renovation plan has been estimated for each ore pass providing a great support for mine planners to create highly reliable long-term production plans. Adjiski et al. [5] used the discrete element method (DEM) to analyze ore pass system configurations. A total of nine scenarios have been simulated considering different geometric parameters of ore pass and material flow in order to recognize potential damage zones and to minimize the hang-ups and wall degradation. Hadjigeorgiou et al. [6] presented two case studies at Brunswick mine, in Canada, relating to an examination of the influence of structural design parameters on ore pass systems. In the first case study, ore pass system degradation is caused by the complex rock structure surrounding the ore pass, while in the second case study, an ore pass system is exposed to the combined influence of high-stress conditions prevailing in a monitored mining zone and the high-velocity of material flow through the ore pass. Chen et al. [7] developed a new plugging technology based on a composite bar combined casing with pre-stressed cables for a collapsed ore pass. A detailed analysis and the effects of building up the applied plugging system for a destroyed main ore pass is demonstrated in the case study of the Xingshan Iron Mine in China. Esmaieli et al. [8] analyzed the stability of the ore pass at Brunswick mine in Canada. The paper is based on analysis of the high stress and material flow as two critical factors influencing the structural stability of the ore pass as well as its useful life. Gardner and Fernandes [9] showed an analysis of the ore pass rehabilitation through the three case studies from Impala Platinum Limited. They concluded that ore pass deterioration is primarily caused by complex geological conditions and stress regime governing in the ore deposit. Greberg et al. [10] evaluated the possible options of a haulage system in an underground mine in Sweden as a case study. By using discrete event simulation, the haul truck transportation system is analyzed as an alternative variant of ore pass for the rock mass transportation at an underground sublevel caving mine method. Li et al. [11] presented the optimization of an underground mine transportation system based on the wolf colony algorithm. The paper demonstrated the transportation route of the mining equipment and optimized the total tonnage of the mined ore from seven stopes to the two ore passes. A similar study is represented by Hou et al. [12] in the underground gold mine in Shandong Province, China. In this paper, transportation routes containing six stopes and two ore passes are illustrated using a simulation model where the number of loaders and trucks are optimized. Koivisto [13] provided an exhaustive analysis of the ore pass design including longevity, inclination, dimension, support, material flow, ore pass rehabilitation, etc., in Kittilä Mine as a case study. Also, Koivisto analyzed the problem of ore pass location selection by simulating different scenarios of the optimal ore pass location, in which Scenario 1 was accepted as the most economically sustainable solution.

Bearing in mind the importance of this problem, we developed an optimization model to enable mining engineers to design the most efficient ore pass system. The mining business is burdened by many uncertainties which are primary related to the investment and production costs. To quantify these uncertainties, we apply the concept of fuzzy theory,

i.e., the concept of triangular fuzzy numbers. The optimization model is composed of the two components. The first component refers to the fuzzy cost objective function, which should be minimized, while the second component refers to the set of techno-dynamic constraints that must be met. According to the previously mentioned facts, our problem can be classified as a fuzzy 0–1 linear programming model. To reduce the complexity of the fuzzy environment, within linear programming, we transform the fuzzy objective function into a crisp one. The transformation is based on the novel Torricelli–Simpson ranking function. A prerequisite to apply the Torricelli–Simpson ranking function relates to the normalization of the original triangular fuzzy number. It includes normalization of the smallest, most promising, and largest values, respectively. Also, the value of the membership function of the most promising value must be normalized. The normalized triangular fuzzy number is now treated as a triangular graph, composed of vertices and edges. The Torricelli point is a single point, which lies within a triangular graph, whose total Euclidean distance from the normalized values, excluding the normalized most promising value, is minimal. The Torricelli point represents an intersection of Simpson lines, and its x-coordinate is a crisp value of the normalized triangular fuzzy number. The crisp value of the original triangular fuzzy number is obtained via the inverse process of normalization. The Torricelli–Simpson ranking function creates the crisp 0–1 linear programming environment, and the ore passes optimization problem can be solved via existing methods.

A comparison with some of the existing defuzzification methods has shown that the novel method can create a crisp value of a triangular fuzzy number with a high level of reliability. The stability analysis shows stable results regardless of whether the triangular fuzzy number is symmetric or non-symmetric. Accordingly, the developed ranking function is capable of being used in the creation of the crisp value of a triangular fuzzy number.

The Torricelli–Simpson ranking function is also capable of ranking symmetric triangular fuzzy numbers with equal modes and different spreads. Additional capability relates to the ranking of symmetric triangular fuzzy numbers with equal modes but with different membership functions.

The efficiency of the proposed ore pass system optimization model is evaluated on the hypothetical ore deposit, where the sublevel method is applied as a means of underground mining. To the best of the authors' knowledge, this is the first optimization model for an underground mine ore pass system. Because of that, we are unable to compare the existing models and highlight their limitations. Currently, underground mine designers locate ore passes primarily based on previous experience without the use of any support tools. The hypothetical case study took into account all possible combinations between a finite set of stopes and ore pass locations. Accordingly, the model is characterized by high level of precision (accuracy).

The proposed methodology has several advantages which can be highlighted as follows:

- Novel method of defuzzification of triangular fuzzy numbers;
- Ranking of the special types of triangular fuzzy numbers;
- Optimal number of ore passes from the finite set of potential ore pass locations;
- Optimal locations of ore passes from the finite set of potential ore pass locations;
- Optimal plan of ore transportation from stopes to ore passes;
- Provision of support to mining engineers in the process of designing underground mines.

Sensitivity analysis, which considers the changes in ore transportation costs, shows the sensitivity of the developed model toward the direction of increasing the number of ore passes as the costs rise.

The paper is organized as follows. Section 1 comprises the Introduction and a brief literature review as well as the main objectives of the developed model. The transformation of a triangular fuzzy number into a crisp (non-fuzzy) number via the Torricelli–Simpson ranking function is extensively described in Section 2. An ore pass system optimization model for sublevel mining is illustrated in Section 3, with special attention given to the

fuzzy objective function of the developed model. Section 4 relates to a numerical example, the obtained results of which are comprehensively described therein. A sensitivity analysis of the model is presented in Section 5, while the concluding remarks and directions of future research are discussed in Section 6.

2. From Fuzzy to Crisp Linear Programming Model via Torricelli–Simpson Ranking Function

The classical 0–1 linear programming aims to minimize (maximize) an objective function subject to a finite set of linear constraints, where variables take a value of 0 or 1. The problem is formulated in the following way:

$$\begin{aligned} &\min f = cx, \\ &\text{s.t.} Ax \leq b, \\ &x \in [0,1]. \end{aligned} \tag{1}$$

where $c^T = (c_1, c_2, \ldots, c_n)^T \in R^n$ presents the cost (benefit) vector, $x = (x_1, x_2, \ldots, x_n)^T \in \mathbb{R}^n$ is a vector of variables, $b = (b_1, b_2, \ldots, b_n)^T \in \mathbb{R}^m$ is a vector of right-hand-side constraint coefficients, and $A = \left[a_{ij}\right]_{m \times n} \in R^{m \times n}$ is a matrix of left-hand-side constraint coefficients.

The presented formulation of 0–1 linear programming is one of the common methods used to find out the best solution for different optimization problems, with assumptions that all coefficients are crisp in nature. However, real-world problems are inaccurate and implicit. Therefore, coefficient uncertainties must be considered, and a triangular fuzzy number (TFN) is very suitable and useful for it. Triangular fuzzy numbers belong to fuzzy theory, which defines the concept of membership function to express the uncertainty of variables [14]. A membership function is defined by the degree of acceptance of a variable as a member of the fuzzy set A; $\mu_{\tilde{A}}(x) : X \to [0,1]$.

Definition 1. *A triangular fuzzy number $\tilde{A} = (a, b, c)$ is defined as a triplet, where a, b and c are the smallest, most promising, and largest values, respectively. The membership function of TFN has the following conditions:*

$$\mu_{\tilde{A}}(x) = \begin{cases} 0, & x \leq a, \\ \frac{x-a}{b-a}, & a \leq x \leq b, \\ \frac{c-x}{c-b}, & b \leq x \leq c, \\ 0, & x \geq c. \end{cases} \tag{2}$$

A plot of a common TFN is presented in Figure 1.

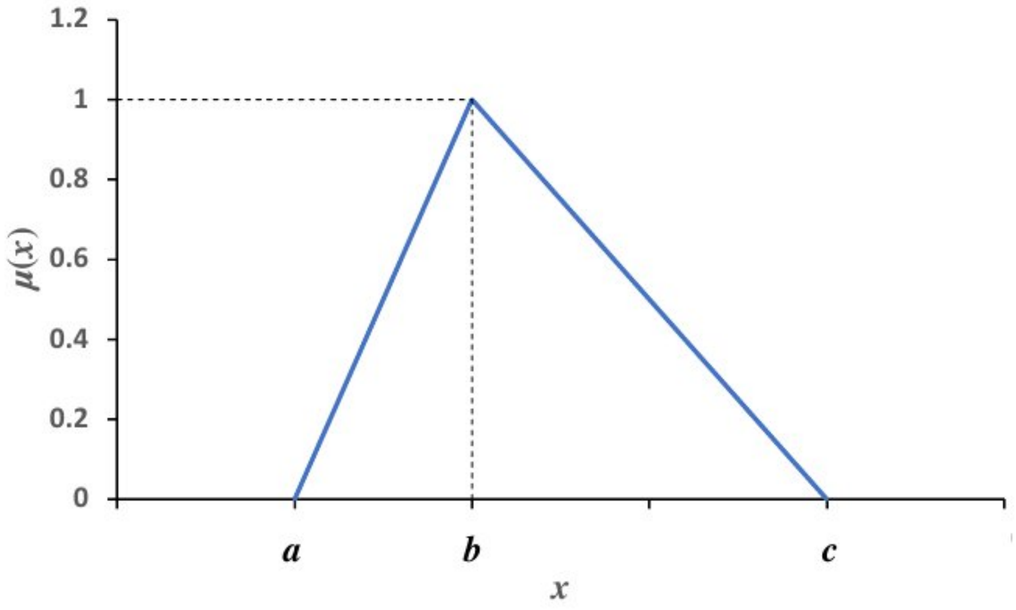

Figure 1. A triangular fuzzy number.

So, a fuzzy 0–1 linear programming model is performed based upon Equation (1), and is as follows:

$$\begin{aligned} &\min \widetilde{f} = \widetilde{c}x, \\ &\text{s.t.} \widetilde{A}x \leq \widetilde{b}, \\ &x \in [0,1]. \end{aligned} \tag{3}$$

Further, a triangular fuzzy number can be presented as an artificial triplet (a, b, c) with the following characteristics:

$$\begin{cases} a < 1, \\ b < 1, \\ c < 1. \end{cases} \tag{4}$$

A triangular fuzzy number with previously characteristics can be created by normalization.

Definition 2. *A normalized triangular fuzzy number (NTFN) is defined as follows:*

$$\mu_{\widetilde{A}_N}(x) = \begin{cases} 0, & x \leq a_N, \\ \frac{x-a_N}{b_N-a_N}, & a_N \leq x \leq b_N, \\ \frac{c_N-x}{c_N-b_N}, & b_N \leq x \leq c_N, \\ 0, & x \geq c_N. \end{cases} \tag{5}$$

where a_N, b_N and c_N are the smallest, most promising, and largest normalized values, respectively. The membership function of TFN must also be transformed. The normalized values of a triplet (a, b, c) and the transformed membership function are calculated in the following way:

$$\widetilde{A}_N = \begin{cases} a_N = \frac{a}{\sqrt{a^2+b^2+c^2}}, & \mu(a_N) = 0, \\ b_N = \frac{b}{\sqrt{a^2+b^2+c^2}}, & \mu(b_N) = 1 + \frac{n+1}{n}, \\ c_N = \frac{c}{\sqrt{a^2+b^2+c^2}}, & \mu(c_N) = 0. \end{cases} \tag{6}$$

where n is a triplet ($n = 3$). An example of normalization is presented in Figure 2.

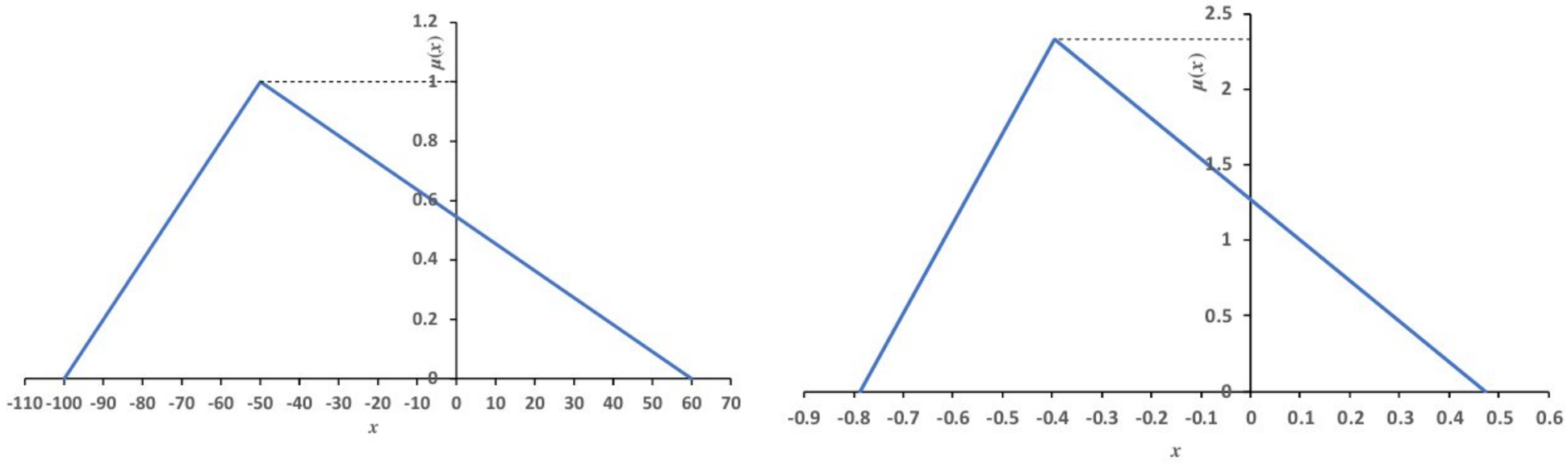

Figure 2. Transformation of TFN to NTFN.

Normalization is a prerequisite for the application of the Torricelli–Simpson ranking function (TSRF) in solving a fuzzy 0–1 linear problem. The concept of a ranking function is closely related to the method of defuzzification of a TFN. A ranking function (RF) converts a fuzzy problem into a crisp one, and it maps each TFN into the real line, RF = TFN $\overset{map}{\rightarrow} \mathbb{R}$. Different approaches of a RF exist. Yager proposed a ranking function which converts fuzzy numbers over the unit interval [15]. Chen ranked fuzzy numbers by minimizing the set and maximizing the set [16]. Wang applied an integral value to rank fuzzy numbers [17]. Adamo proposed the decision trees method as a ranking function for data expressed by a common language whose semantic representations are fuzzy numbers [18]. González

developed the general ranking function approach as a ranking process using a mean value and an interval relation [19]. Chutia developed a ranking technique which uses the notion of value and a multiple of an ambiguity inclusion–exclusion function [20]. Duta proposed a sophisticated ranking method based on the concept of the exponential area of the fuzzy numbers [21]. Zou et al. ranked fuzzy numbers via a two-dimensional Monte Carlo simulation technique [22]. Wang and Mo introduced left and right deviation degree of fuzzy numbers as measure of fuzziness, which is the global attribute of fuzzy numbers [23]. Pourabdollah et al. created a close-form formula for alpha-cut defuzzification that involves both the membership function and its derivative [24]. Asady and Zendehnam defuzzified fuzzy numbers using a minimizer of the distance between the two fuzzy numbers [25].

Consider NTFN, and denote triangle vertex as V_i $(x_i, \mu(x_i))$, $i = 1,2,3$, where x_i is a value of fuzzy event and $\mu(x_i)$ is a transformed membership function of event (see Figure 3). The coordinates of the vertices are: V_1 $(a_N,0)$, V_2 $(b_N,1 + 1.333)$ and V_3 $(c_N,0)$.

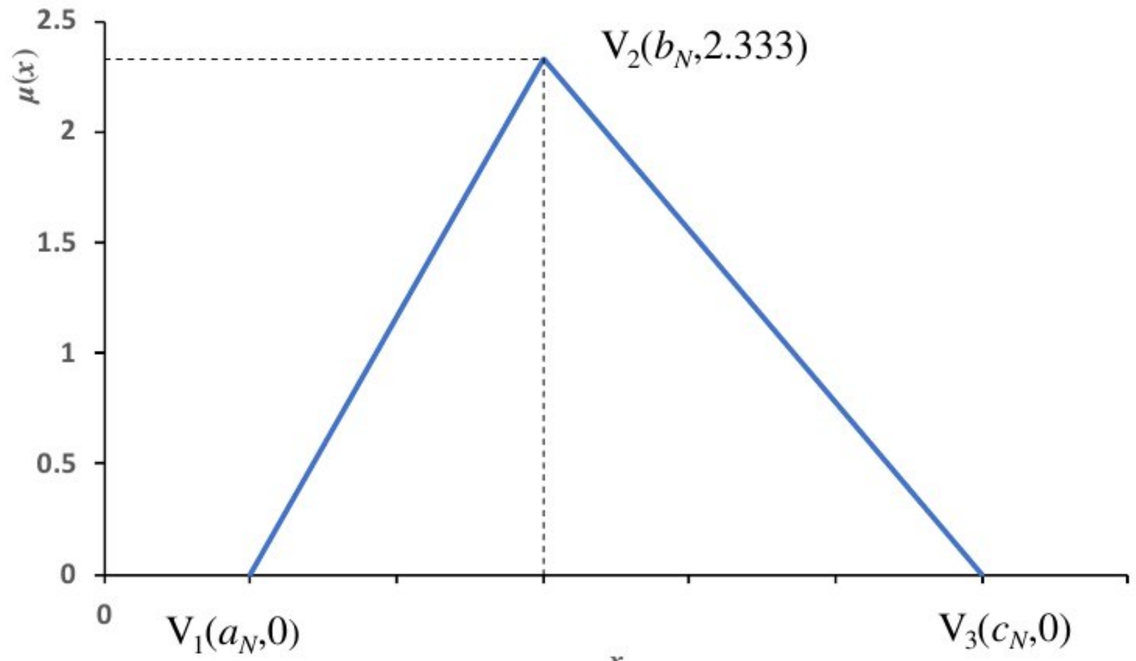

Figure 3. Coordinates of NTFN vertices.

Definition 3. *NTFN is a graph* G = (V, E), *where* V *and* E *present a set of vertices and a set of edges, respectively.*

Each edge connects a pair of vertices. Another term for a graph defined in this way is a network. In Figure 3, we have V = {V_1, V_2, V_3} and E = {e_1, e_2, e_3}. Edge e_1 connects vertices V_1 and V_2, edge e_2 connects V_1 and V_3, and edge e_3 connects V_2 and V_3.

The Euclidean Steiner tree problem looks for a network of minimal total length which spans over a given set N composed of n points in the Euclidean plane. Brasil et al. [26] described the Euclidean Steiner tree problem in the following way.

Definition 4. *Find a geometric network* T = (V, E) *such that* $N \subseteq V$ *and* $S = V \backslash N$ *is a set of points known as Steiner points, and such that* $\sum_{e \in E}|e|$ *is minimal.*

The origins of the Euclidean Steiner tree problem are closely related to the Fermat–Torricelli problem, which can be thought of as the simplest non-trivial case of the Steiner problem for $n = 3$. The problem is to find a single point in the plane whose total Euclidean distance from three given points is minimal. The Italian physicist and mathematician Evangelista Torricelli solved the problem in a geometric way. The method can be formulated as follows:

- Start by joining the three points in the plane to form a triangle;
- Construct three equilateral triangles, one on each edge of the original triangle;
- Construct three circles circumscribing each equilateral triangle.

The point at which all circles intersect is known as the Torricelli point (T). The Simpson method works by drawing a Simpson line from each vertex of the equilateral triangles, which do not belong to the original triangle, to the opposite vertex, which belongs to the

original triangle. The Simpson lines also intersect at the Torricelli point. The obtained point lies inside a triangle and has exactly three incident edges meeting at 120° degree angles. Neither of these methods works properly if any of the angles of an original triangle are larger than 120°. This is the main reason we created NTFN. Through the normalization of TFN, we avoid such a situation, and all angles of NTFN are smaller than 120°. The construction of the Torricelli point of NTFN, via both methods, is presented in Figure 4.

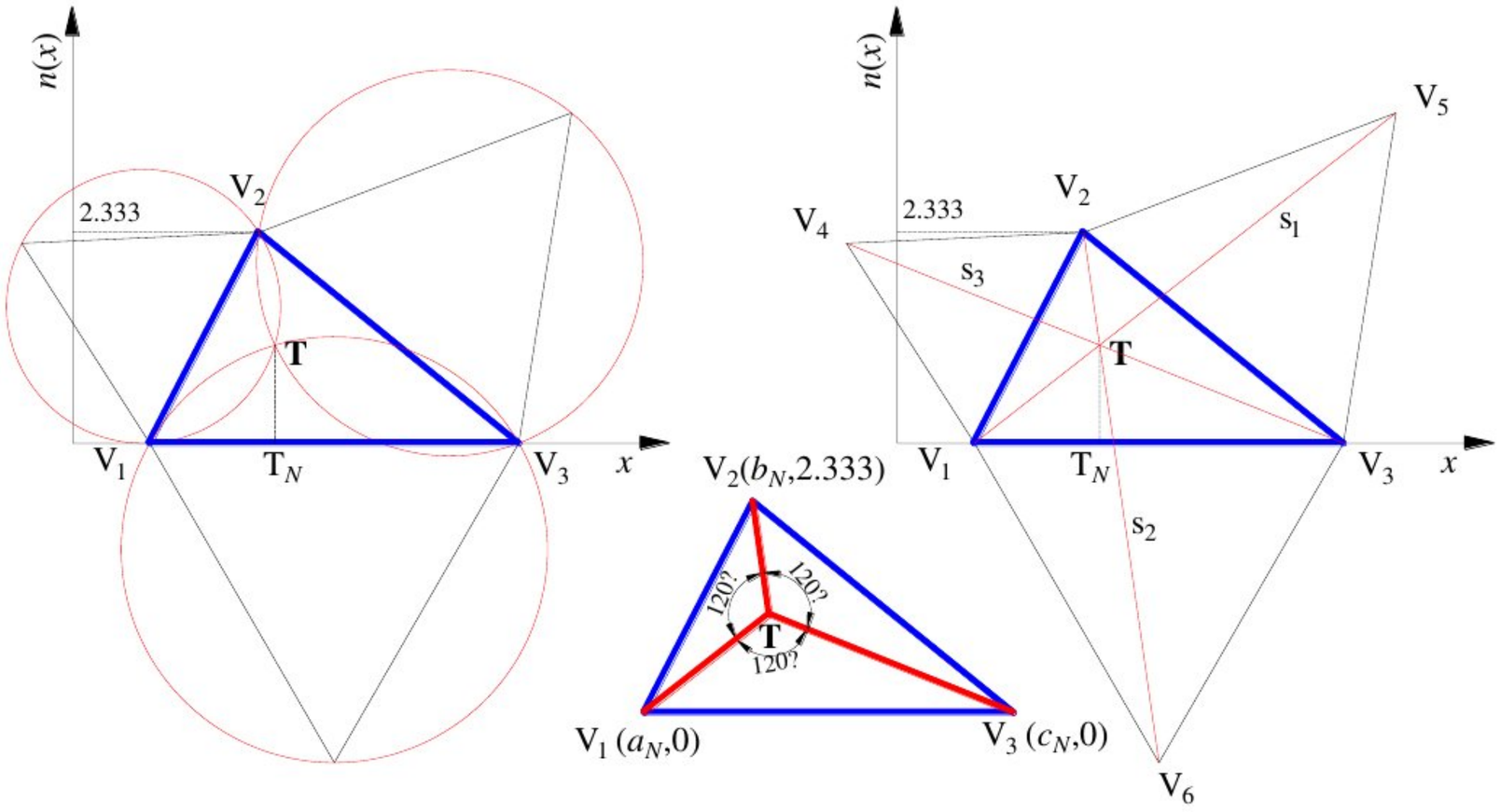

Figure 4. Application of Torricelli and Simpson geometric methods for NTFN.

Normalized coordinates of the Torricelli point are T (TN, μ(TN)). The algebraic method for solving the Torricelli point problem, based on the geometric solution, is composed of the following steps in succession:

Step 1. Calculate the coordinates of a vertex V_4,
Step 2. Obtain an equation of Simpson line s_3, which connects vertex V_4 and vertex V_3,
Step 3. Calculate the coordinates of a vertex V_6,
Step 4. Obtain an equation of Simpson line s_2, which connects vertex V_6 and vertex V_2,
Step 5. Find the intersection of the two Simpson lines, s_3 and s_2.

Step 1. Vertex V_4 presents an intersection of lines l_1 and l_2 (see Figure 5). For simplicity, we use standard notation for coordinates, x and y, although y = μ(x). A gradient (slope) of a line l_1 equals:

$$\begin{cases} g_1 = \tan\left(60 + \arctan\left(\frac{2.333}{|b_N - a_N|}\right)\right), \\ \arctan\left(\frac{2.333}{|b_N - a_N|}\right) = 90, \text{if } a_N = b_N. \end{cases} \quad (7)$$

The equation of line l_1, which has a gradient of g_1 and passes through a vertex $V_1(a_N,0)$, is:

$$l_1 : y = g_1(x - a_N) = \tan\left(60 + \arctan\left(\frac{2.333}{|b_N - a_N|}\right)\right)(x - a_N), \quad (8)$$

A gradient of line l_2 equals:

$$\begin{cases} g_2 = \tan\left(30 - \arctan\left(\frac{|b_N - a_N|}{2.333}\right)\right), \\ \arctan\left(\frac{|b_N - a_N|}{2.333}\right) = 0, \text{if } a_N = b_N. \end{cases} \quad (9)$$

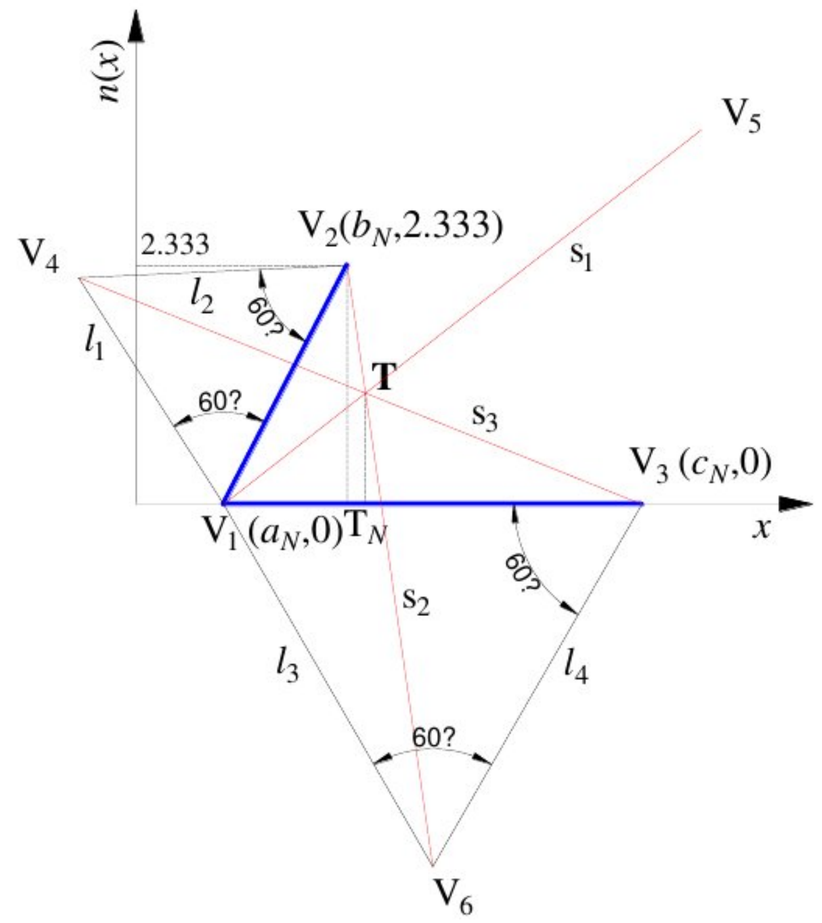

Figure 5. Vertices V_4 and V_6 as intersections of two lines.

The equation of line l_2, which has a gradient of g_2 and passes through a vertex V_2 (b_N, 2.333), is:

$$l_2 : y = g_2(x - b_N) + 2.333 = \tan\left(30 - \arctan\left(\frac{|b_N - a_N|}{2.333}\right)\right)(x - b_N) + 2.333, \quad (10)$$

The coordinates of vertex V_4 are as follows:

$$V_4(x_4, y_4) = V_4\left(\frac{g_1 a_N - g_2 b_N + 2.333}{g_1 - g_2}, g_1\left(\frac{g_1 a_N - g_2 b_N + 2.333}{g_1 - g_2} - a_N\right)\right), \quad (11)$$

Step 2. The equation of the Simpson line s_3, which passes through two vertices, V_4 and V_3, is as follows:

$$s_3 : y = \frac{-g_1\left(\frac{g_1 a_N - g_2 b_N + 2.333}{g_1 - g_2} - a_N\right)}{c_N - \frac{g_1 a_N - g_2 b_N + 2.333}{g_1 - g_2}}\left(x - \frac{g_1 a_N - g_2 b_N + 2.333}{g_1 - g_2}\right) + g_1\left(\frac{g_1 a_N - g_2 b_N + 2.333}{g_1 - g_2} - a_N\right), \quad (12)$$

Step 3. Vertex V_6 presents an intersection of lines l_3 and l_4 (see Figure 5). The gradients of lines l_3 and l_4 are: $g_3 = \tan(120) = -\sqrt{3}$ and $g_4 = \tan(60) = \sqrt{3}$; so, the equations of lines l_3 and l_4 are as follows:

$$l_3 : y = -\sqrt{3}(x - a_N), \quad (13)$$

$$l_4 : y = \sqrt{3}(x - c_N), \quad (14)$$

The coordinates of vertex V_6 are as follows:

$$V_6(x_6, y_6) = V_6\left(\frac{a_N + c_N}{2}, \sqrt{3}\left(\frac{a_N - c_N}{2}\right)\right), \quad (15)$$

Step 4. The equation of the Simpson line s_2, which passes through two vertices V_6 and V_2, is as follows:

$$s_2 : y = \frac{2.333 - \sqrt{3}\left(\frac{a_N - c_N}{2}\right)}{b_N - \frac{a_N + c_N}{2}}\left(x - \frac{a_N + c_N}{2}\right) + \sqrt{3}\left(\frac{a_N - c_N}{2}\right); s_2 : x = b_N, if\ b_N - a_N = c_N - b_N, \quad (16)$$

Step 5. As we mentioned, the intersection of Simpson lines creates the Torricelli point. Let us introduce new notations to simplify searching for the coordinates of intersection:

$$s_3 : y = \omega_3(x - \varphi_3) + \delta_3, \tag{17}$$

$$s_2 : y = \omega_2(x - \varphi_2) + \delta_2, \tag{18}$$

Solving the system of Equations (17) and (18), we obtain the following x-coordinate of the Torricelli point of NTFN as follows:

$$T_N = \frac{\omega_3\varphi_3 - \omega_2\varphi_2 + \delta_2 - \delta_3}{\omega_3 - \omega_2}, \tag{19}$$

where:

$$\omega_3 = \frac{-g_1\left(\frac{g_1a_N - g_2b_N + 2.333}{g_1 - g_2} - a_N\right)}{c_N - \frac{g_1a_N - g_2b_N + 2.333}{g_1 - g_2}} \quad \varphi_3 = \frac{g_1a_N - g_2b_N + 2.333}{g_1 - g_2} \quad \delta_3 = g_1\left(\frac{g_1a_N - g_2b_N + 2.333}{g_1 - g_2} - a_N\right), \tag{20}$$

$$\omega_2 = \frac{2.333 - \sqrt{3}\left(\frac{a_N - c_N}{2}\right)}{b_N - \frac{a_N + c_N}{2}} \quad \varphi_2 = \frac{a_N + c_N}{2} \quad \delta_2 = \sqrt{3}\left(\frac{a_N - c_N}{2}\right), \tag{21}$$

The single number or crisp value of TFN based on the Torricelli–Simpson ranking function (TSRF) is calculated as follows:

$$\mathrm{TSRF}\left(\widetilde{A}\right) = T_N \cdot \sqrt{a^2 + b^2 + c^2}, \tag{22}$$

The additional benefits of the Torricelli–Simpson ranking function are presented in the Appendix A section. The TSRF is capable of ranking triangular fuzzy numbers which have the same mode but different symmetric spreads. It is also capable of ranking triangular fuzzy numbers with different values of the membership function.

Let us consider the second part of Equation (16), $s_2 : x = b_N, if\ b_N - a_N = c_N - b_N$. Obviously, it is a symmetric TFN, and we used that to simplify the calculation of the Torricelli–Simpson ranking function.

Simplification means searching for the intersection between line s_2 and the x-axis only. The intersection between Simpson line $s_2 : y = \frac{2.333 - \sqrt{3}\left(\frac{a_N - c_N}{2}\right)}{b_N - \frac{a_N + c_N}{2}}\left(x - \frac{a_N + c_N}{2}\right) + \sqrt{3}\left(\frac{a_N - c_N}{2}\right)$ and x-axis is defined as follows:

$$S_N = \frac{A \cdot B - C}{A}, \tag{23}$$

where:

$$A = \frac{2.333 - \sqrt{3}\left(\frac{a_N - c_N}{2}\right)}{b_N - \frac{a_N + c_N}{2}}; B = \frac{a_N + c_N}{2}; C = \sqrt{3}\left(\frac{a_N - c_N}{2}\right), \tag{24}$$

Now, the crisp value of the TFN is calculated as follows and shown in Figure 6.

$$\mathrm{SRF}\left(\widetilde{A}\right) = S_N \cdot \sqrt{a^2 + b^2 + c^2}, \tag{25}$$

To solve the problem defined by Equation (3), we transform it into an equivalent crisp form, replacing the fuzzy objective function and fuzzy constraints with:

$$\begin{aligned} &\min f = \mathrm{deff}\left(\widetilde{c}\right)x, \\ &\text{s.t.}\mathrm{deff}\left(\widetilde{A}\right)x \le \mathrm{deff}\left(\widetilde{b}\right), \\ &x \in [0, 1]. \end{aligned} \tag{26}$$

where abbreviation "deff" denotes the defuzzified value of TFN; and the Torricelli–Simpson or Simpson ranking function is TSRF$\left(\widetilde{A}\right)$ or SRF$\left(\widetilde{A}\right)$, respectively. The crisp problem is now solved by using standard linear programming methods.

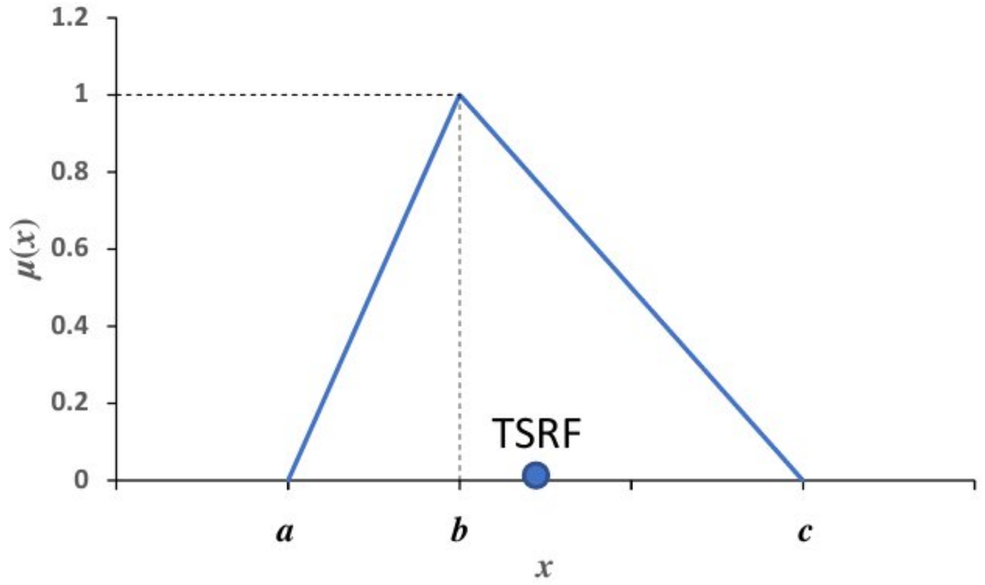

Figure 6. Torricelli–Simpson ranking function of TFN.

3. Ore Passes Optimization Model for Sublevel Mining

3.1. Sublevel Mining

Sublevel mining is an underground mining method which is intended for the excavation of deeply situated massive orebodies. The orebody is divided into vertical intervals through horizontal openings called production drifts. So, a sublevel is a vertical section of the orebody which is limited, with two production drifts on various neighboring levels. A sublevel drift is driven along to the strike of an orebody, and it is in the footwall. The main purpose of a sublevel drift is to connect production drifts and provide ore transportation from stopes to ore passes, and it also performs the ventilation of stopes. Ore passes are positioned along the strike of the ore body in the vicinity to the sublevel drift. Several sublevels make up one mining horizon, and one main haulage drift is assigned to each horizon. Mining activities start at the uppermost sublevel of the mining horizon and proceed sequentially downward to the lowest sublevel of the mining horizon. The main haulage level is directly located below the lowest sublevel. Hence, the mining front advances toward the main haulage drift, while in each sublevel, the mining front advances from hanging wall to the footwall, toward the sublevel drift. In each sublevel, the ore is drilled in a fan-shaped pattern along the production drift at the constant horizontal distance, called the burden. Then, holes drilled into ore are filled with explosives for blasting. Load haul dump equipment is used to transport blasted ore from stopes to the ore passes. This sequence of activities is repeated in a cyclical way. From the bottom of each ore pass, ore is transported along the main haulage level to the main conveyance system and further to the surface [27–30].

3.2. The Model

An ore pass is a vertical or near-vertical opening, which is created during underground mining operations, through which ore falls under gravity to the lowest designed level. Before formulating the underground ore passes optimization problem, a number of things are assumed, and these are:

- Access system to the ore body is designed;
- Mining method parameters are defined;
- Sublevel access system is designed;
- Mining plan is defined;
- Set of potential ore pass locations is finite;
- Circular-shaped ore pass with adequate cross-sectional dimensions (area) is adopted;
- Safe distance between two operating ore passes is defined.

In the optimization problem of the ore pass system, we firstly form the objective function. It describes the required problems by suitable equations. This is followed by setting up a goal, which can be maximal or minimal, in the spirit of an objective function. In finding the feasible solution, there are technical requirements (constraints) that must be met, and the constraints are expressed by a set of equations. Ore pass system optimization can be treated as a location–allocation problem. This is a strategic decision-making problem concerning the selection of the best subset of ore passes from a set of potential locations and the allocation of quantities of mined ore to the selected locations, over a defined period. An inefficient solution to the problem can lead to a bottleneck in production and can severely affect the mining business.

Suppose there is an ore pass which connects production sublevels and enables ore to fall from each sublevel to the main haulage level. The following operations are closely related to the ore pass system organization:

- Operation 1: blasted ore is transported from a stope to the dumping point by the load–haul–dump vehicle (see Figure 7). The ore is hauled through the production drift.
- Operation 2: at the dumping point, ore is dumped into an ore pass and ends up at the loading point, which is located at the bottom of an ore pass, near the haulage drift.
- Operation 3: at the loading point, ore is also loaded by a loader and hauled to the main transportation system. The ore is hauled through the main haulage drift (see Figure 8).

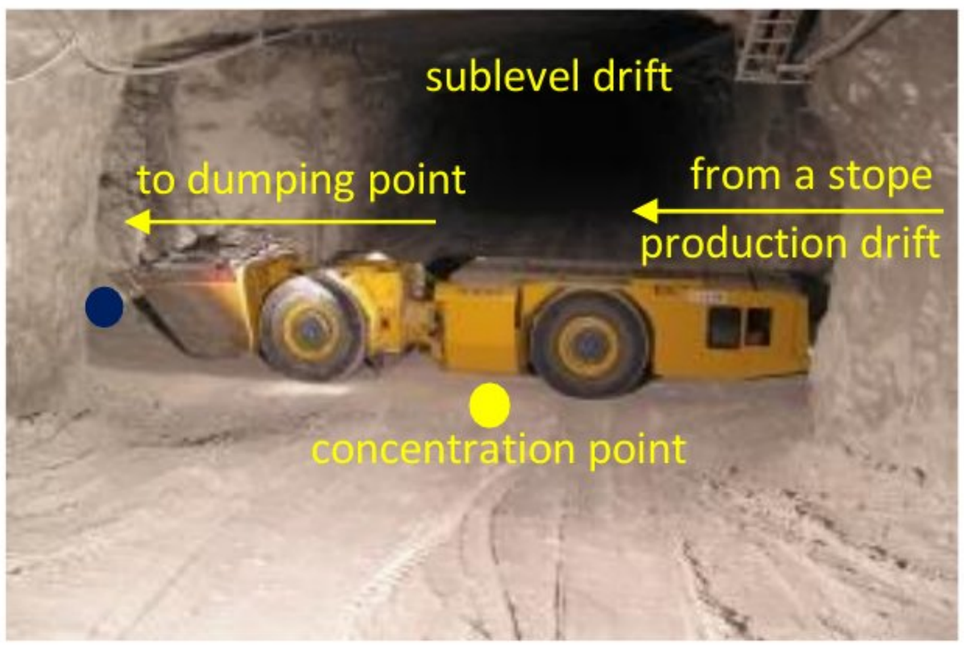

Figure 7. Load–haul–dump (LHD) vehicle in operation on sublevel; figure adopted from [31] and transformed.

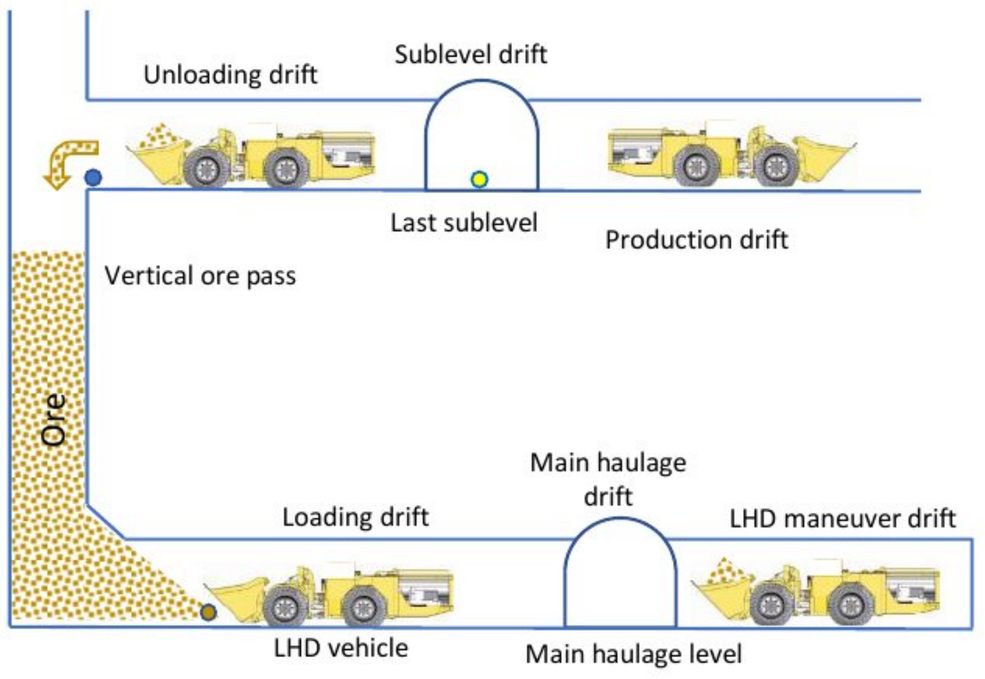

Figure 8. Operations relating to an ore pass.

The concentration point is a point where the sublevel drift and stope production drift cross each other, and where the entire quantity of ore from a stope is concentrated. Note that this is an artificial point which is defined only for the purpose of optimization, and the ore is not dumped at this point. It can be treated as a center of gravity of a stope. The

section concentration point (SCP) is the center of gravity of a stope part, which should be mined out according to a mining plan.

Graph theory is a capable concept which helps us to understand the ore passes optimization problem by visualization. As the first step, we present the vertical cross-section, longitudinal cross section and horizontal cross-section of an ore pass system in Figures 9–11, respectively. Cross-sections contain the position of sublevels; possible mining plan on sublevels; ore pass positions; location of concentration points and dumping and loading points; positions of production and sublevel drifts; and position of the main haulage drift. The unloading drift is a section of production drift between the concentration and dumping point, while the LHD maneuver drift is a section of the loading drift. Usually, the loading and main haulage drift intersect at a right angle.

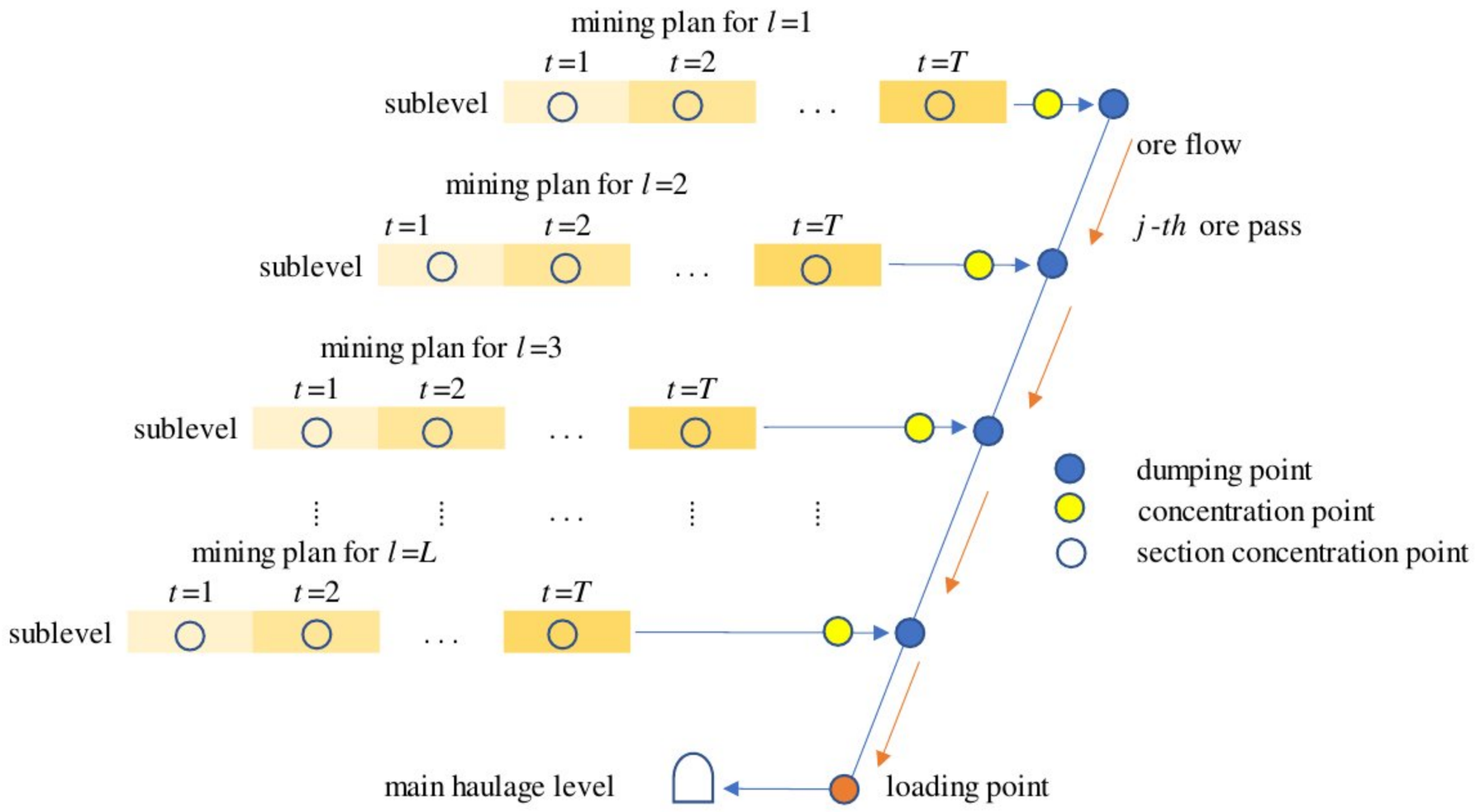

Figure 9. Vertical cross section of an ore pass.

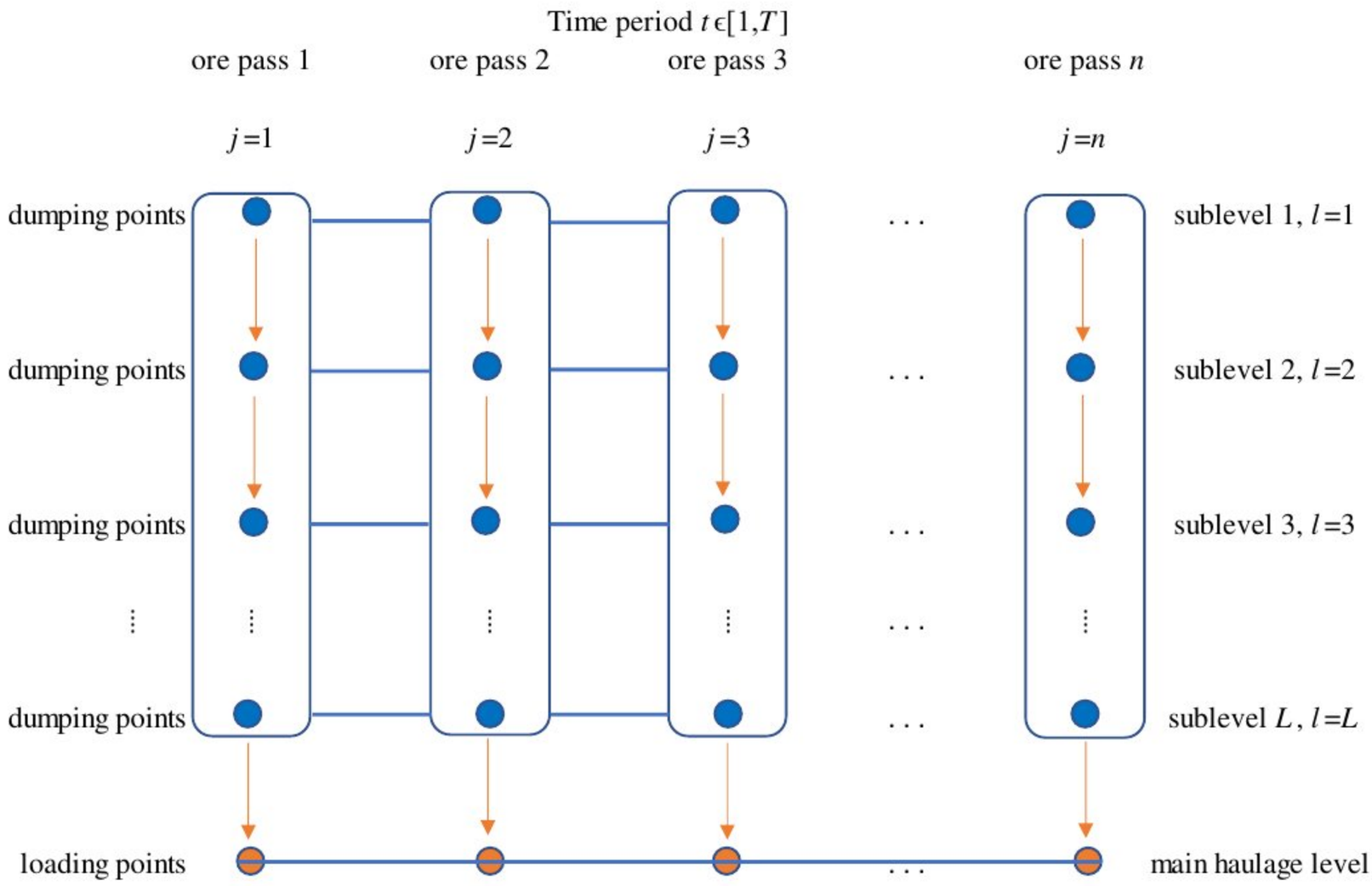

Figure 10. Longitudinal cross section of ore pass system.

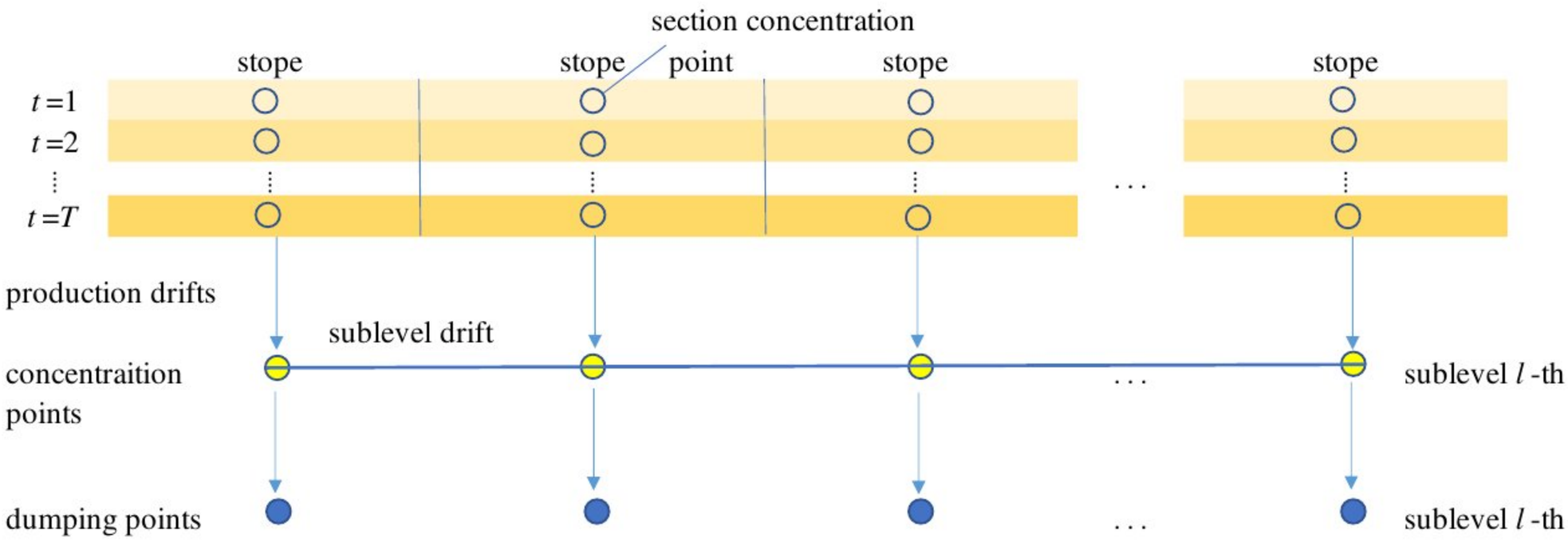

Figure 11. Horizontal cross-section of ore pass system on sublevel.

Since the concentration point and dumping point are neighboring points, a potential set of ore pass locations is then equal to a set of concentration points. According to the terminology of location–allocation methodology, ore passes are candidate points. The location of ore passes on the candidate sites and the assignment of mined ore to each located ore pass are determined such that the total cost is minimized. The total cost is the sum of the transportation costs and costs of ore pass excavation (development). An ore pass is usually excavated via the drill and blast method. A graph of the ore pass location–allocation problem is shown in Figure 12.

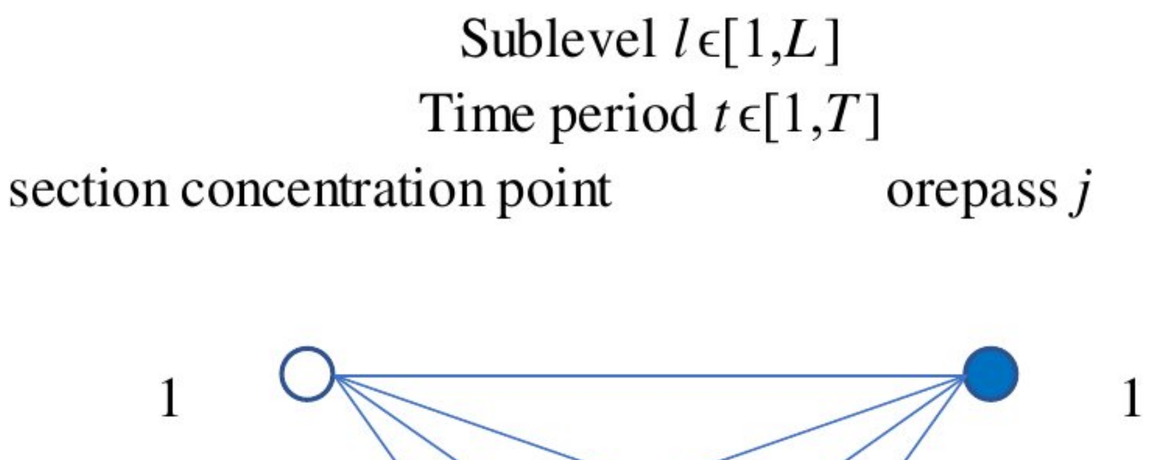

Figure 12. A graph of the ore passes optimization problem.

The optimization problem can be presented by a graph denoted as G (V, E), where V is a finite set of vertices, and E is a finite set of edges. Set V consists of ore pass candidate points, while set E consists of haulage drift sections. Vertices are weighted by ore pass development costs, and edges are weighted by ore transportation costs. The problem is to

find a subset $K \subseteq$ V of ore passes as to minimize the total cost. The outcome of the problem is the number of selected ore passes as well as their locations and ore tonnage assignment plan over time.

Accordingly, the fuzzy objective function, which is aimed at minimizing the total cost of the ore pass system, is as follows:

$$\widetilde{F} = \sum_{i=1}^{m} \sum_{j=1}^{n} \sum_{t=1}^{T} \sum_{l=1}^{L} r_{i,t,l} \widetilde{c}_t d_{ij,t,l} x_{ij,t,l} + \sum_{j=1}^{n} \widetilde{C}_j x_j \rightarrow \min, \tag{27}$$

subject to:

$$\sum_{i=1}^{m} x_{ij,t,l} = 1, \forall j \in [1,n], \forall t \in [1,T], \forall l \in [1,L], \tag{28}$$

$$x_{ij,t} - x_{j,t} \leq 0, \forall i \in [1,m], \forall j \in [1,n], \forall t \in [1,T], \forall l \in [1,L], \tag{29}$$

$$\sum_{t=1}^{T} x_{ij,l+1} - \sum_{t=1}^{T} x_{ij,l} \leq 0, \forall i \in [1,m], \forall j \in [1,n], \forall l \in [1,L-1], \tag{30}$$

$$x_{ij,t,l} + x^{s}_{ij,t,l} \leq 1, \forall i \in [1,m], i = j, \forall s \in [1,S], \forall t \in [1,T], \forall l \in [1,L], \tag{31}$$

$$x_{ij} + x^{s}_{ij} \leq 1, \forall i \in [1,m], i = j, \forall s \in [1,S], \tag{32}$$

$$x_{ij,t,l} - x_j \leq 0, \forall i \in [1,m], i = j, \forall t \in [1,T], \forall l \in [1,L], \tag{33}$$

$$x_{ij,t,l} \in [0,1]; x_j \in [0,1]. \tag{34}$$

where the following are defined:

m—total number of section concentration points;

n—total number of ore pass candidate points;

$r_{i,t,l}$—tonnage of ore which gravitates to the i-th section concentration point on the l-th sublevel in time t;

$\widetilde{c}_t$—fuzzy unit transportation costs in time t;

$d_{ij,t,l}$—distance between the i-th section concentration point and the j-th candidate point on the l-th sublevel in time t;

L—total number of sublevels;

T—mining time;

S—a set of candidate points that do not meet the safe distance condition relative to j-th candidate point;

$\widetilde{C}_j$—fuzzy cost of ore passes excavation (development);

$x_{ij,t,l}$—binary variable;

x_j—binary variable.

In underground mining practice, ore pass excavation is called ore pass development. Ore pass development through the rock massive is accomplished via drilling and blasting. Information on rock mass properties is gathered by surface exploration drilling with sampling. A wide-space grid pattern of drilling and testing of the rock core samples is used, and information on rock mass characteristics between bore holes is gathered by interpolation. Hence, we cannot define the properties of rock mass at a micro-location, where the ore pass should be developed, with high level precision. It may be that the full length of the ore pass, or some sections, must be supported by rebar and liners, such as shotcrete. It is a source of uncertainties, and triangular fuzzy numbers are a very convenient way to quantify cost uncertainties. Transportation equipment operating costs are also burdened with uncertainties, due to adjustments in inputs such as labor, fuel, lubricants, tires and spare parts. The market price of these inputs is explicitly defined by

the business strategy of suppliers. To protect themselves, suppliers are offering short-term contracts to mines, which is in contrast to traditional long-term contracts. This is one of the reasons why we use triangular fuzzy numbers to express ore transportation costs.

In some cases, alternative fuzzy set types, such as Interval Type-2 Fuzzy Sets (IT2FS), may be required to capture more complex or higher-order uncertainty patterns. The choice of fuzzy set type depends on the specific characteristics of the uncertainty being modeled and the requirements of the application at hand. But, in this case study, TFNs have shown stable and rational results.

We have implemented TFNs in this study due to several reasons:

- TFNs are useful when data availability is limited or uncertain, which is the case in this study. In this study, obtaining precise data for uncertainty modeling was challenging, and TFNs enable experts to represent and reason about uncertainty based on their knowledge, experience or imprecise data.
- TFNs are computationally efficient compared to more complex fuzzy set types such as interval type-2 fuzzy sets. The calculations involving TFNs are less demanding in terms of computational resources. This efficiency facilitates quicker linear programming and decision-making processes.
- One of the contributions of this study is the proposal of a new methodology for the defuzzification of fuzzy numbers. To present the mentioned idea, the authors decided to apply TFNs. This paper presents a novel approach for the defuzzification of TFNs using the Torricelli–Simpson ranking function. In the following research, the author's intention is to show the possibilities of applying the Torricelli–Simpson ranking function for the defuzzification of trapezoidal fuzzy numbers and other types of uncertainty.
- Our intention is to develop a decision support system based on the developed methodology. To achieve this goal, we need a stable system with easily integrated parts. TFNs can be easily integrated into real-world decision support systems and processes. They can be used alongside traditional crisp or deterministic values, providing a seamless transition from conventional methods to fuzzy-based approaches without major disruptions.

The objective function (27) of the ore pass system model minimizes the total costs, including the ore transportation costs from a stope to an ore pass and the fixed costs of ore pass excavation. Equation (28) implies that total ore tonnage must be transported from a stope (section concentration point) to one ore pass only. Constraint (29) and constraint (30) do not allow discontinuity or segmentation of the ore pass.

The continuity of the ore pass must be achieved, from the first sublevel to the main haulage level.

Constraints (31), (32) and (33) relate to the pillar thickness between two operating ore passes. We named this thickness as safety distance D. The aim of this constraint is to select locations of ore passes with no stress interaction between them. Having created numerical stress modeling, Bunker et al. showed the mechanism of stress interaction (see Figure 13) and proposed a minimum safety distance of 30 m [32].

Members of set S are defined in the following way:

$$\begin{cases} 1, \text{if } d_{j,j+h,t,l} < D \rightarrow s \in S, \forall j \in [1,n], \forall h \in [1,2,\ldots,n-j], \forall t \in [1,T], \forall l \in [1,L], \\ 0, \text{if } d_{j,j+h,t,l} \geq D \rightarrow s \notin S, \forall j \in [1,n], \forall h \in [1,2,\ldots,n-j], \forall t \in [1,T], \forall l \in [1,L]. \end{cases} \quad (35)$$

Constraint (34) strictly supports the following statements:

- If variable $x_{ij,t,l}$ takes a value of 1, then the ore is transported from i-th section concentration point to the j-th ore pass on the l-th sublevel in time t, otherwise 0;
- If the ore pass is excavated in location j, then variable x_j takes a value of 1, otherwise 0.

Figure 14 shows a flowchart of the ore passes optimization model.

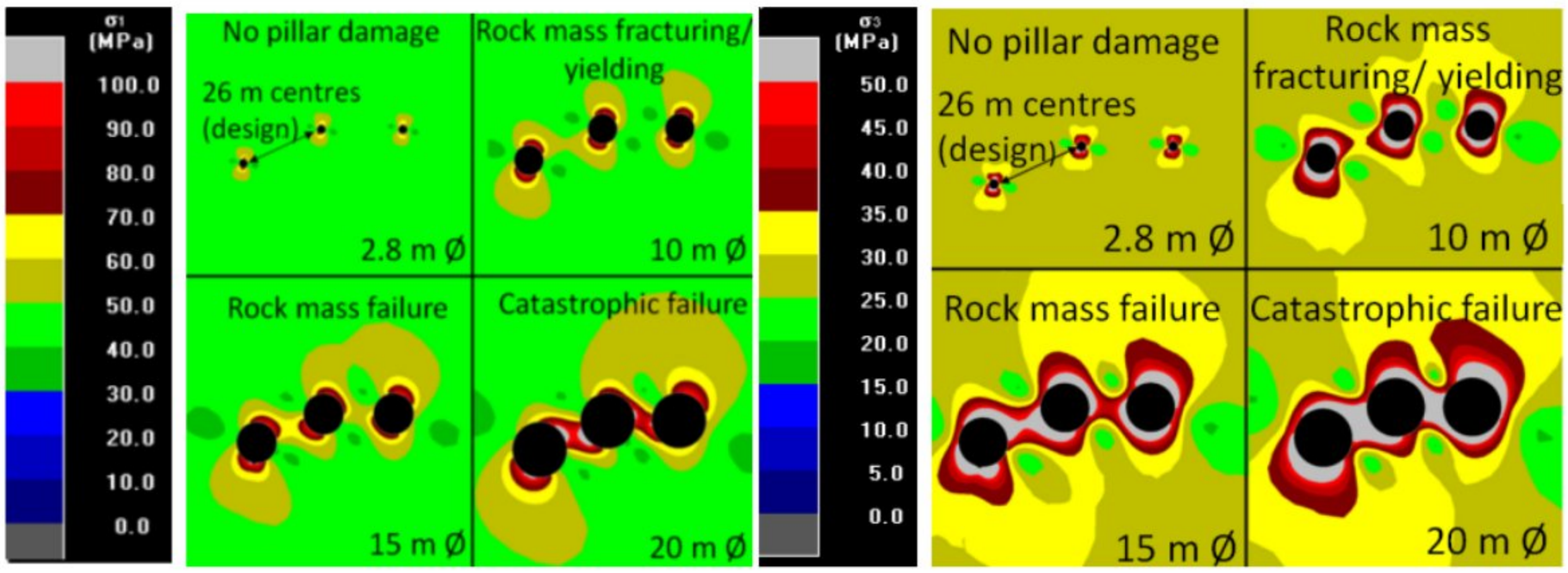

Figure 13. Vertical raise interaction (**left**) and deviatoric (**right**) stress results.

Fuzzy objective function of ore passes system:

$$\tilde{F} = \sum_{i=1}^{m}\sum_{j=1}^{n}\sum_{t=1}^{T}\sum_{l=1}^{L} r_{i,t,l}\,\tilde{c}_t d_{ij,t,l} x_{ij,t,l} + \sum_{j=1}^{n} \tilde{C}_j\, x_j \rightarrow \min$$

Deffuzification of fuzzy objective function of ore passes system by the novel Torricelli-Simpson ranking function (TSRF) method:

$$F = \sum_{i=1}^{m}\sum_{j=1}^{n}\sum_{t=1}^{T}\sum_{l=1}^{L} r_{i,t,l}\, c_t d_{ij,t,l} x_{ij,t,l} + \sum_{j=1}^{n} C_j\, x_j \rightarrow \min$$

Creation a set of techno-dynamic constraints

$$\sum_{i=1}^{m} x_{ij,t,l} = 1, \forall j \in [1,n], \forall t \in [1,T], \forall l \in [1,L]$$

$$x_{ij,t} - x_{j,t} \leq 0, \forall i \in [1,m], \forall j \in [1,n], \forall t \in [1,T], \forall l \in [1,L]$$

$$\sum_{t=1}^{T} x_{ij,l+1} - \sum_{t=1}^{T} x_{ij,l} \leq 0, \forall i \in [1,m], \forall j \in [1,n], \forall l \in [1,L-1]$$

$$x_{ij,t,l} + x_{ij,t,l}^{s} \leq 1, \forall i \in [1,m], i = j, \forall s \in [1,S], \forall t \in [1,T], \forall l \in [1,L]$$

$$x_{ij} + x_{ij}^{s} \leq 1, \forall i \in [1,m], i = j, \forall s \in [1,S]$$

$$x_{ij,t,l} - x_j \leq 0, \forall i \in [1,m], i = j, \forall t \in [1,T], \forall l \in [1,L]$$

$$x_{ij,t,l} \in [0,1];\ x_j \in [0,1]$$

Optimal solution of ore passes system:

- optimal number of ore passes
- optimal location of ore passes
- optimal dynamic ore transportation plan

Figure 14. Flowchart of the ore passes optimization model.

4. Numerical Example

To evaluate the developed optimization model, we used a hypothetical cooper deposit. The sublevel mining method was selected as a means of underground mining, with the following design parameters and ore characteristics:

- Number of sublevels which was analyzed, 3 sublevels;
- Sublevel height, 15 m;

- Stope width, 10 m;
- Stope height, 15 m;
- Ore pass length, 44 m;
- Ore pass is vertical;
- Cross-section of ore pass is circular, with diameter of 2 m;
- Number of stopes on each sublevel, 20 stopes;
- Total number of stopes, 60 stopes;
- Ore density, 2.65 t/m^3.

The hypothetical cooper deposit and sublevel mining method are presented in Figure 15.

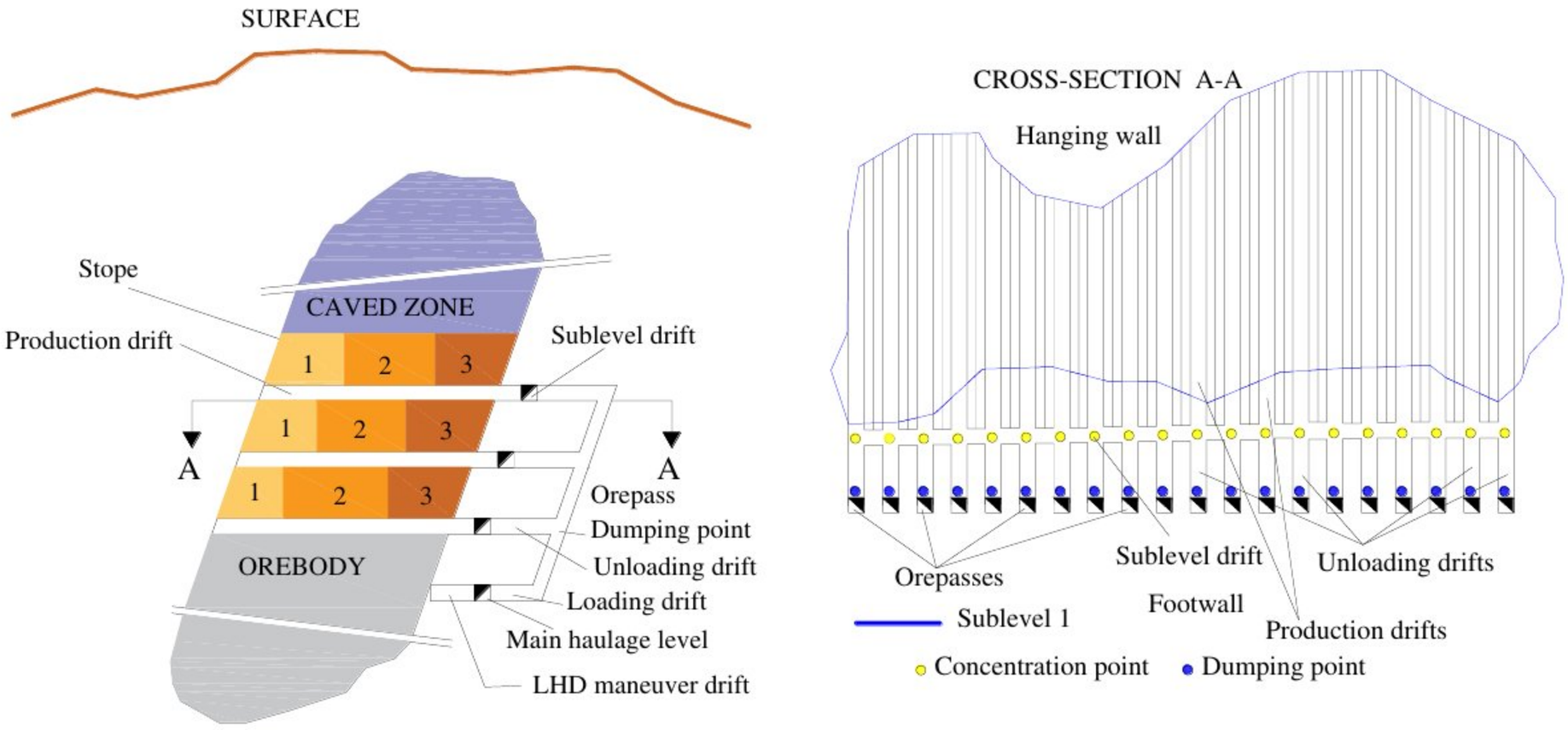

Figure 15. Ore deposit and schematic design of sublevel development.

The sublevel's mining plan is presented in Figure 16 and Table 1. On each sublevel, there are twenty stopes, and each stope is divided into three sections. Colored sections represent the sequencing of the stope with respect to yearly time horizon. The mining plan spans three years for a total production of 882,848 t of ore.

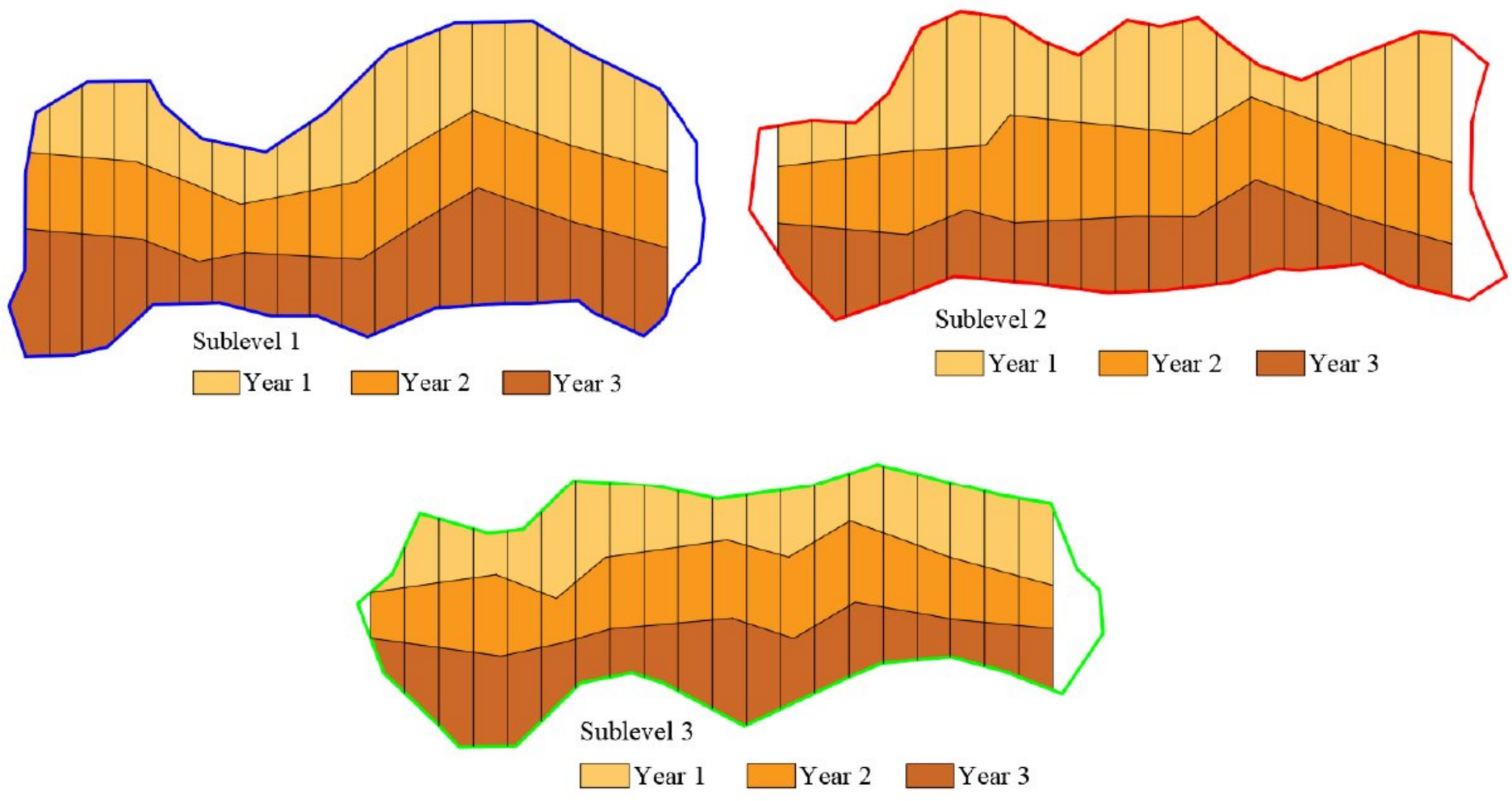

Figure 16. Mining plan on each sublevel.

Table 1. Mining plan on sublevels.

	Sublevel 1			Sublevel 2			Sublevel 3		
	Year 1 (t)	Year 2 (t)	Year 3 (t)	Year 1 (t)	Year 2 (t)	Year 3 (t)	Year 1 (t)	Year 2 (t)	Year 3 (t)
	5605	5247	5804	8030	5247	3419	5247	3021	3697
	6201	5247	6201	7115	5247	3379	5048	3419	3061
	6758	5247	5645	5645	5247	3061	4889	3816	2663
	7314	5207	6002	4055	5247	3737	4850	4253	2783
	7354	5207	6917	2504	5247	4730	4571	4651	3419
	6519	5287	7791	2266	5247	5684	3856	5128	4214
	6678	5525	7314	4015	5565	5645	3498	5525	4571
	7235	5525	6440	6797	5486	4770	4134	5446	4412
	7592	5525	5963	6917	5486	4770	3816	5168	5804
	6917	5366	5247	6758	5724	4850	2981	5088	6440
	5366	4810	4333	5366	6082	4691	3339	5048	5168
	4174	4214	4214	4611	6440	4333	4094	4929	3816
	3538	3657	4134	5446	6758	3975	4691	4810	3101
	3776	3935	3419	7354	5645	4015	5724	4333	3061
	3657	5088	3101	8626	4253	4214	6400	3339	4015
	4889	5207	3896	7910	4850	3935	4015	4253	5605
	5605	5287	6042	4889	5207	4214	2942	5128	6042
	5287	5287	7831	2703	4770	5168	3697	4571	5963
	4214	5287	8467	2544	4333	5406	4134	3935	4174
	1630	3896	8069	2703	3856	3339	994	3299	2067
Total	110,306	100,051	116,825	106,252	105,934	87,331	82,919	89,159	84,071

Summary mining plan is shown in Table 2 and Figure 17.

Table 2. Summary mining plan.

Year/Sublevel	Year 1 (t)	Year 2 (t)	Year 3 (t)
Sublevel 1	110,306	100,051	116,825
Sublevel 2	106,252	105,934	87,331
Sublevel 3	82,919	89,159	84,071
Total	299,477	295,144	288,227

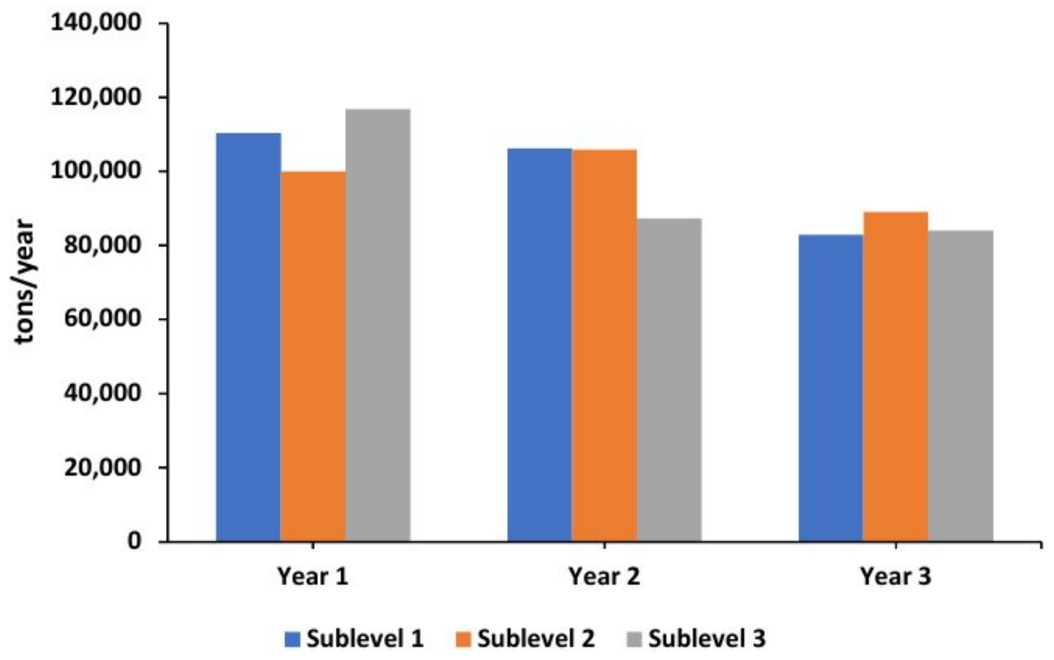

Figure 17. Summary mining plan.

Since production activities are planned, we can create a graph that represents the ore pass system optimization problem. The numbering system which defines the section concentration points (SCP) in ascending order, on each sublevel, is as follows:

- Sublevel 1: SCP 1 is located 54 m from the sublevel drift (upper-right corner). SCP 21 and SCP 41 are located 36 m and 16 m from the sublevel drift, respectively (see Figure 18);

- Sublevel 2: SCP 61 is located 58 m from the sublevel drift (upper-right corner). SCP 81 and SCP 101 are located 36 m and 21 m from the sublevel drift, respectively (see Figure 19);
- Sublevel 3: SCP 121 is located 54 m from the sublevel drift (upper-right corner). SCP 141 and SCP 161 are located 40 m and 19 m from the sublevel drift, respectively (see Figure 20).

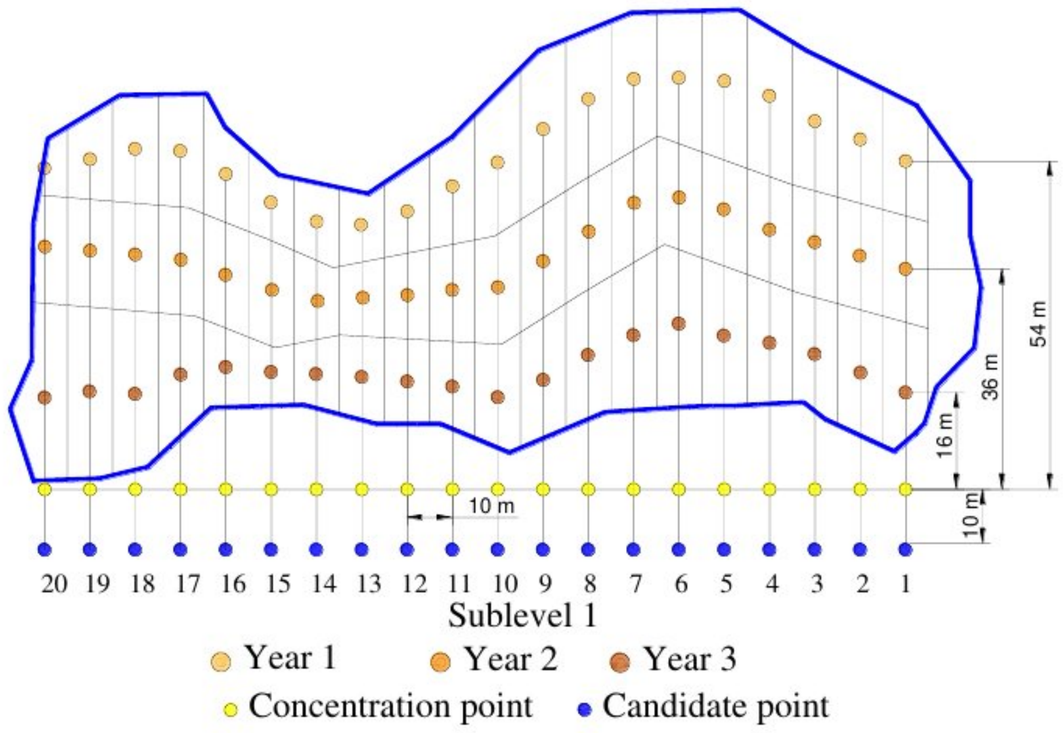

Figure 18. Disposition of characteristic points on sublevel 1.

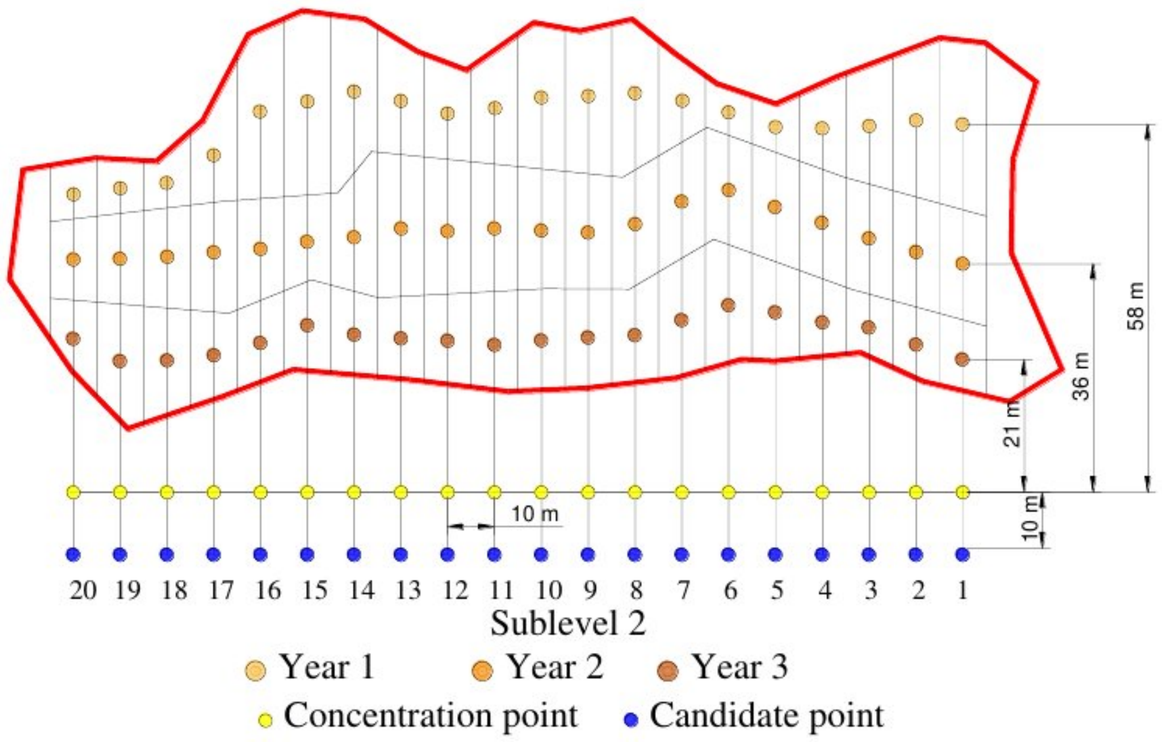

Figure 19. Disposition of characteristic points on sublevel 2.

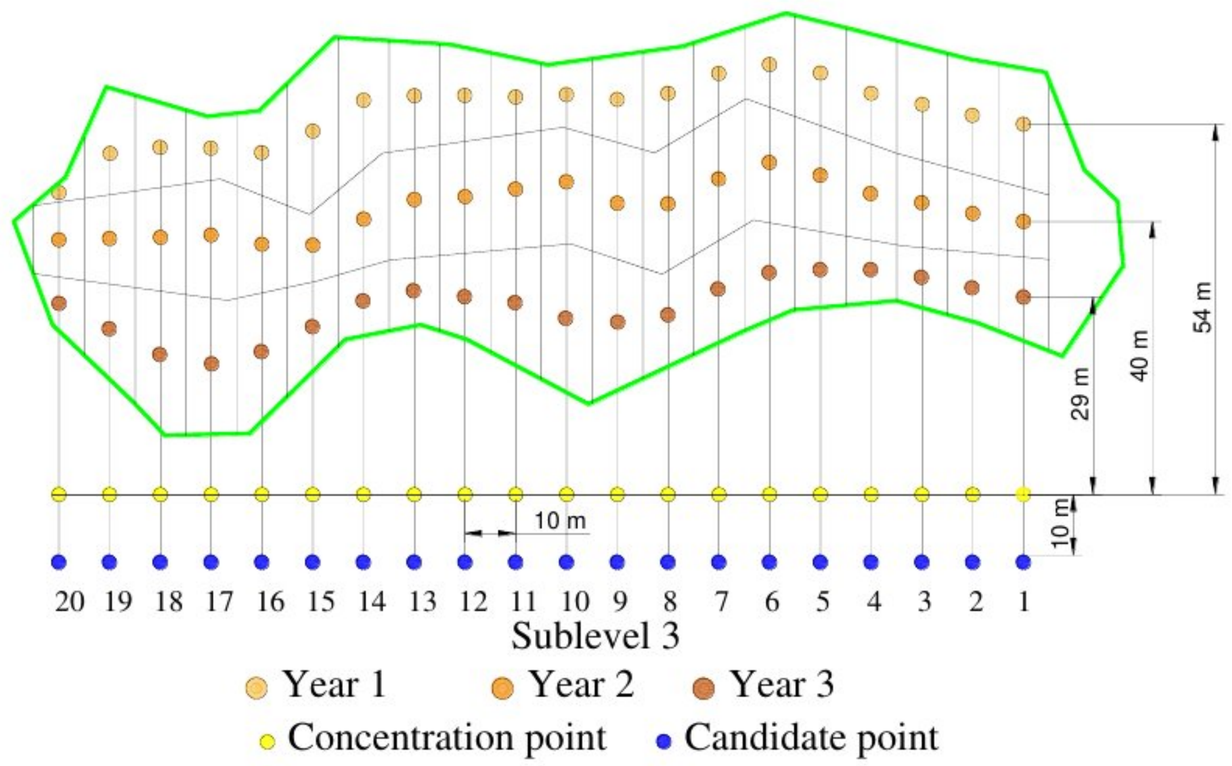

Figure 20. Disposition of characteristic points on sublevel 3.

Accordingly, on each sublevel, there are 60 section concentration points, and in total, there are 180 section concentration points. The location of each SCP is defined by the perpendicular distance from the sublevel drift (see Table 3).

Table 3. Distance between section concentration point and concentration point.

Concentration Point	Sublevel 1			Sublevel 2			Sublevel 3		
	Year 1 (m)	Year 2 (m)	Year 3 (m)	Year 1 (m)	Year 2 (m)	Year 3 (m)	Year 1 (m)	Year 2 (m)	Year 3 (m)
1	54	36	16	58	36	21	54	40	29
2	58	39	19	59	38	23	56	41	30
3	61	41	22	58	40	26	57	43	32
4	65	43	24	58	43	27	59	44	33
5	68	46	25	58	45	28	62	47	33
6	68	48	27	60	48	29	63	49	32
7	68	47	25	62	46	27	62	46	30
8	65	42	22	63	43	25	59	42	26
9	60	37	18	63	41	24	58	43	25
10	54	33	15	61	41	24	59	46	26
11	50	33	17	60	42	23	58	45	28
12	46	32	18	62	41	24	59	44	29
13	43	31	19	65	42	24	59	43	30
14	44	31	19	62	40	25	58	40	28
15	47	33	20	61	40	26	53	37	24
16	52	35	19	54	39	23	50	36	21
17	56	38	16	49	38	21	51	38	19
18	56	39	16	48	37	21	51	37	20
19	54	40	16	47	37	21	50	37	24
20	53	40	15	47	37	25	45	37	28

The numbering system which defines ore passes or candidate points is directed from right to left, in ascending order (see Figures 18–20). The distance between concentration points is 10 m, and the distance between the concentration and candidate point is 10 m. The distance between the SCP and candidate point is calculated by summing up all the sections along the way from the SCP to the candidate point. The following example shows the method of calculating the distance between SCP 10 and candidate point 5 (see Figure 21).

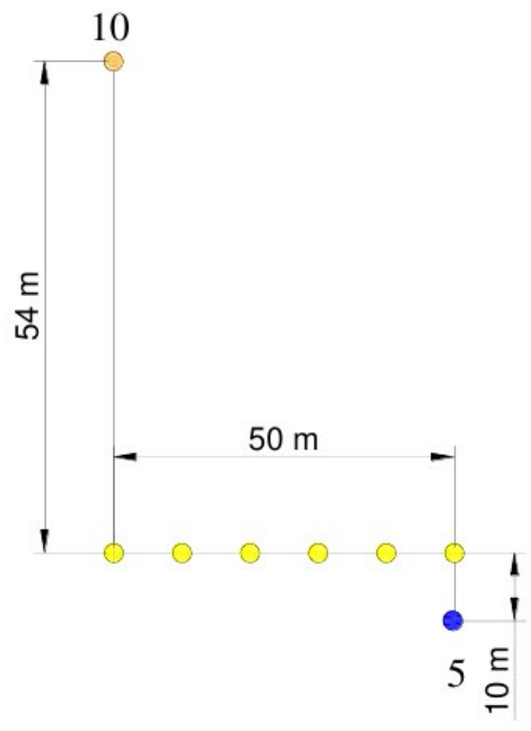

Figure 21. Partial distances between SCP 10 and candidate point 5.

The distance between SCP 10 and candidate point 5 on sublevel 1 in year 1 equals:

$$d_{i=10,j=5,t=1,l=1} = 54 + 50 + 10 = 114\ m, \tag{36}$$

The same approach is used to calculate all distances that exist between the set of section concentration points and set of candidate points. If we take into consideration the presence of $m = 180$ section concentration points and $n = 20$ candidate points, then 3600 distances exist. Obviously, Figure 20 presents the directed graph of the selected example, which describes only geometrical elements of the optimization problem. To obtain a weighted graph, it is necessary to assign costs to edges and vertices. For that purpose, the data set concerning costs is given in Table 4 and in Figures 22 and 23.

Table 4. Cost data.

Cost	Value
Transportation Unit Cost	
Year 1	(0.047 0.049 0.058) USD/t m
Year 2	(0.051 0.057 0.062) USD/t m
Year 3	(0.048 0.052 0.061) USD/t m
Ore pass excavation unit cost	(2270 2550 2750) USD/m
Ore pass length	44 m

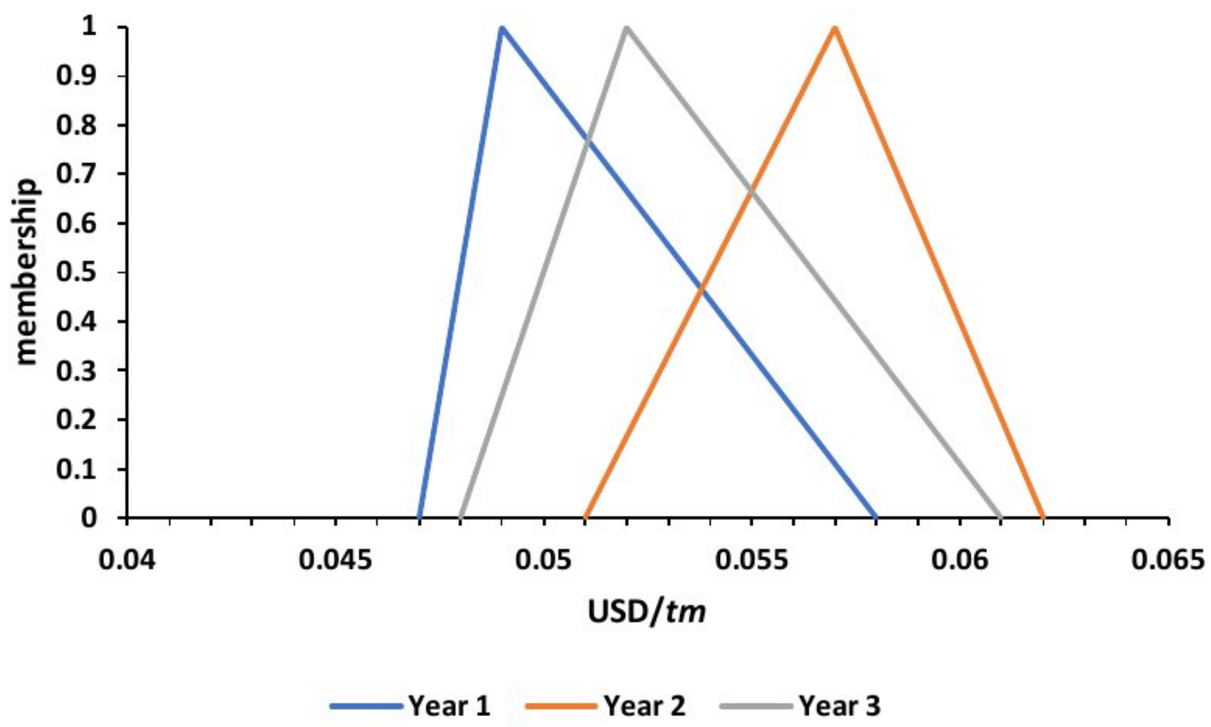

Figure 22. Fuzzy transportation unit cost scenario over time.

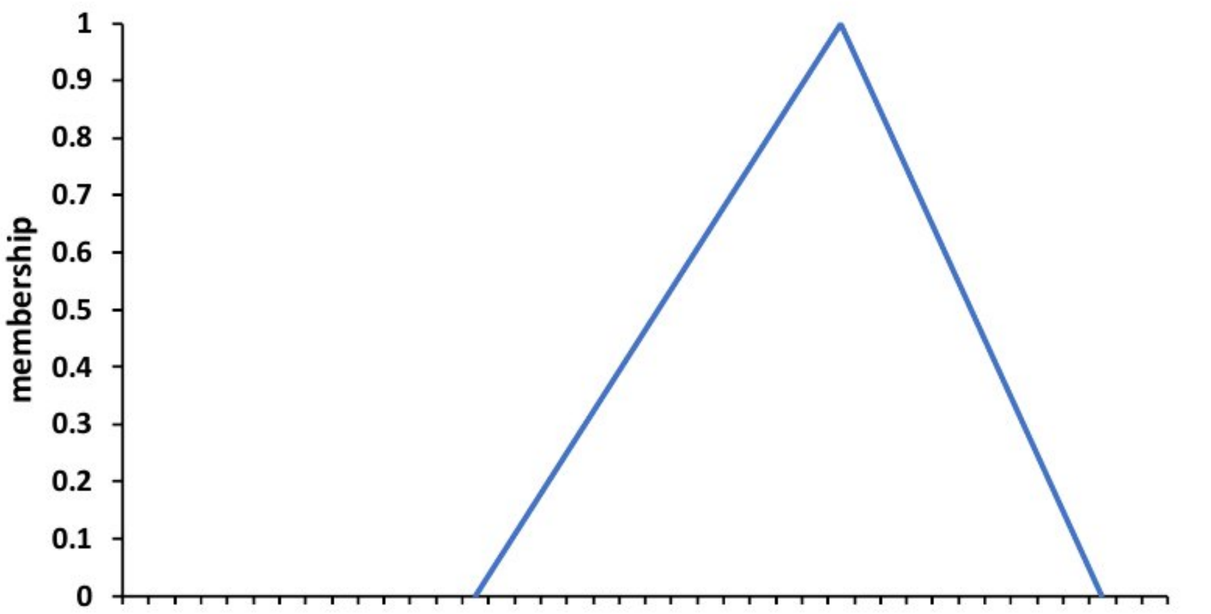

Figure 23. Fuzzy unit cost of ore pass excavation (development).

The combination of SCP 10 and candidate point 5 is also used as an example of the fuzzy coefficient calculation of variable $x_{i=10,j=5,t=1,l=1}$. The value of the fuzzy coefficient for $i = 10$, $j = 5$, $t = 1$, $l = 1$ equals:

$$r_{i,t,l}\widetilde{c}_t d_{ij,t,l} = 6917 \times (0.047\ 0.049\ 0.058) \times 114 = (37,059\ 38,636\ 457,32)\text{USD}, \quad (37)$$

The fuzzy coefficient of variable x_5 equals:

$$\widetilde{C}_5 = 44 \times (2270\ 2550\ 2750) = (99,880\ 112,200\ 121,000)\text{USD}, \tag{38}$$

Equation (37) represents the transportation cost component, while Equation (38) represents the development cost component of the fuzzy objective function. The same calculation is used to define all coefficients in the fuzzy objective function. To solve the problem of ore pass system optimization, it is necessary to transform the objective function from the fuzzy state to the crisp one.

The transportation cost component, which is expressed by triangular fuzzy number $\widetilde{A} = (37,059\ 38,636\ 45,732)$, is used for the presentation of the developed defuzzification method. Applying Equation (6), we obtain normalized triangular fuzzy number as follows.

$$\widetilde{A}_N = \begin{cases} a_N = \frac{37,059}{\sqrt{37,059^2+38,636^2+45,732^2}} = 0.526, & \mu(a_N) = 0 \\ b_N = \frac{38,636}{\sqrt{37,059^2+38,636^2+45,732^2}} = 0.548, & \mu(b_N) = 1 + \frac{3+1}{3}, \\ c_N = \frac{45,732}{\sqrt{37,059^2+38,636^2+45,732^2}} = 0.649, & \mu(c_N) = 0 \end{cases} \tag{39}$$

The value of the fuzzy coefficient for $i = 10$, $j = 5$, $t = 1$ and $l = 1$, and its normalized form is shown in Figure 24.

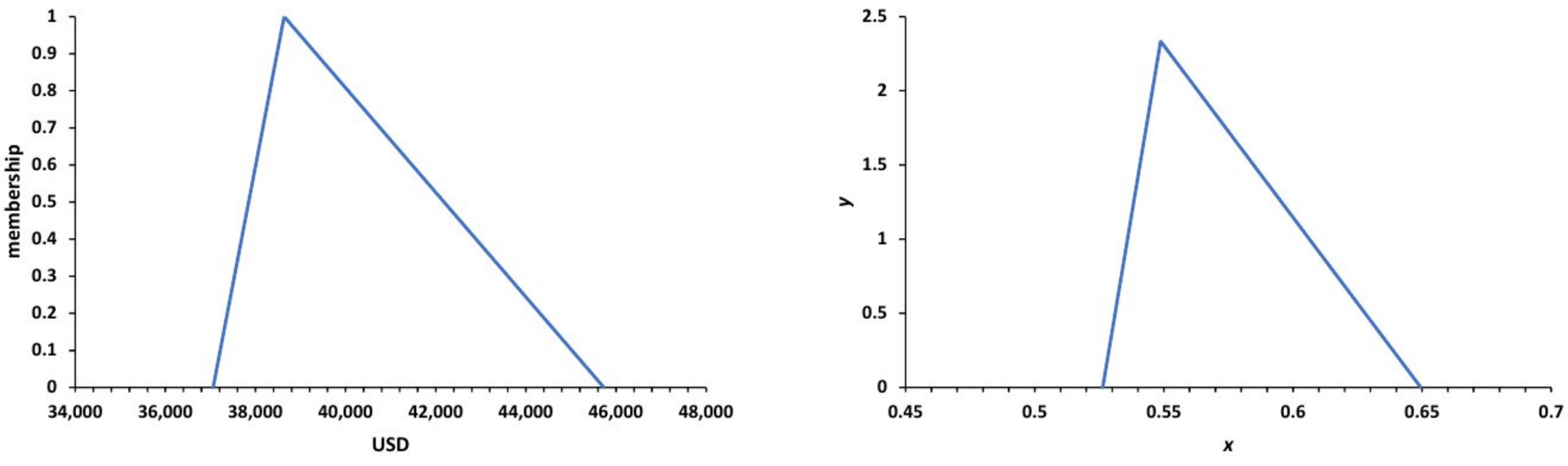

Figure 24. The value of fuzzy coefficient and its normalized form expressed by triangular fuzzy numbers.

According to Figure 4, the coordinates of vertices of the normalized triangular fuzzy number are: $V_1(0.526;0)$, $V_2(0.548;2.333)$ and $V_3(0.649;0)$. The gradient of the line l_1, which passes through the vertex V_1, and its equation are given as follows:

$$g_1 = \tan\left(60 + \arctan\left(\frac{2.333}{|0.548 - 0.526|}\right)\right) = -0.5902, \tag{40}$$

$$l_1 : y = g_1(x - a_N) = -0.5902 \cdot (x - 0.526), \tag{41}$$

The gradient of the line l_2, which passes through the vertex V_2, and its equation are:

$$g_2 = \tan\left(30 - \arctan\left(\frac{|0.548 - 0.526|}{2.333}\right)\right) = 0.5646, \tag{42}$$

$$l_2 : y = g_2(x - b_N) + 2.333 = 0.5646 \cdot (x - 0.548) + 2.333, \tag{43}$$

The coordinates of the vertex, which lies at the intersection of lines l_1 and l_2, are $V_4(-1.483;1.186)$. So, the equation of the Simpson line s_3, which passes through vertices V_4 and V_3, is as follows:

$$s_3 : y = -0.5561 \cdot (x + 1.483) + 1.186, \tag{44}$$

The equations of lines l_3 and l_4, which pass through vertices V_1 and V_3, respectively, are as follows:

$$l_3 : y = -\sqrt{3}(x - a_N) = -\sqrt{3}(x - 0.526), \tag{45}$$

$$l_4 : y = \sqrt{3}(x - c_N) = \sqrt{3}(x - 0.649), \tag{46}$$

The coordinates of the vertex, which lies at the intersection of lines l_3 and l_4, are $V_6(0.587; -0.106)$. Accordingly, the equation of the Simpson line s_2, which passes through vertices V_6 and V_2, is:

$$s_2 : y = \frac{2.333 - \sqrt{3}\left(\frac{a_N - c_N}{2}\right)}{b_N - \frac{a_N + c_N}{2}}\left(x - \frac{a_N + c_N}{2}\right) + \sqrt{3}\left(\frac{a_N - c_N}{2}\right) = -62.2578 \cdot (x - 0.587) - 0.106, \tag{47}$$

The solution of the system of Equations (44) and (47) presents the x-coordinate of the Torricelli point of the normalized triangular fuzzy number $\widetilde{A}_N = (0.526\ 0.548\ 0.649)$, $T_N = 0.585$.

The crisp value of the original triangular fuzzy number $\widetilde{A} = (37,059\ 38,636\ 45,732)$ based on the Torricelli–Simpson ranking function (TSRF) is as follows:

$$\mathrm{TSRF}\left(\widetilde{A}\right) = T_N \cdot \sqrt{a^2 + b^2 + c^2} = 0.585 \cdot \sqrt{37,059^2 + 38,636^2 + 45,732^2} = 41,235 \text{ USD}, \tag{48}$$

The intersection between the Simpson line $s_2 : y = -62.2578 \cdot (x - 0.587) - 0.106$ and the x-axis defines a point with the following x coordinate, $S_N = 0.586$. Now, the crisp value of $\widetilde{A}_N = (0.526\ 0.548\ 0.649)$ based on the Simpson ranking function (SRF) is:

$$\mathrm{SRF}\left(\widetilde{A}\right) = S_N \cdot \sqrt{a^2 + b^2 + c^2} = 0.586 \cdot \sqrt{37,059^2 + 38,636^2 + 45,732^2} = 41,275 \text{ USD}, \tag{49}$$

Applying either the TSRF or SRF approach, we obtain crisp values of each coefficient, which are represented by variables $x_{ij,t,l}$ and x_j, respectively. Through this method, the original fuzzy objective function is transformed into a crisp one, and it can be solved by using any standard linear programming methods.

The validation of the developed method was carried out on the example that we borrowed from Garrido et al. [33]. The example considered the problem of economic benefit maximization generated by tourists with respect to several socio-environmental constraints. The results are shown in Table 5.

Table 5. Validation of proposed methodology.

Ranking Function	$\widetilde{c}_1$=(190,210,230)	$\widetilde{c}_2$=(140,160,180)	$\widetilde{c}_1$=(45,60,80)
Center of gravity	210	160	61.66
Yager's F1	210	160	61.67
Yager's F3	210	160	61.25
Adamo	220	170	70
Campos	216.67	113.33	45
Gonzales	209.57	160	61.67
TSRF	210	160	62.14
SRF	210	160	62.23

To assess the stability of the presented defuzzification techniques (TSRF and SRF), the change in parameters of the fuzzy number $\widetilde{c}_1 = (190, 210, 230)$ was simulated. Since it is

a symmetric fuzzy number where the deviation of the left and right boundaries from the modal value is equal, the defuzzified number is expected to be close to the modal value. Therefore, in the following part, the change in left, modal and right parameters is simulated to generate non-symmetrical parameters of the triangular fuzzy number. The simulation involved ten thousand iterations and was carried out through two phases:

1. In the first phase, a simulated change was performed in the right boundary of the fuzzy number $\widetilde{c}_1 = (190, 210, 230)$, while the left boundary and the modal value remained unchanged. The right border is increased by one in each iteration, so in the last iteration, the right border is increased by ten thousand.
2. In the second phase, the change in all three parameters of the fuzzy number $\widetilde{c}_1$ was simulated as follows: the left value was increased by one in each iteration, the modal value was increased by two times, and the right value was increased by six times in each iteration compared to the previous iteration.

The results obtained in the first and second phases of the simulation were compared using the COG defuzzification technique. Figure 25 compares the defuzzification techniques TSRF, SRF and COG during the first and second phases of the simulation (Figure 25a,b).

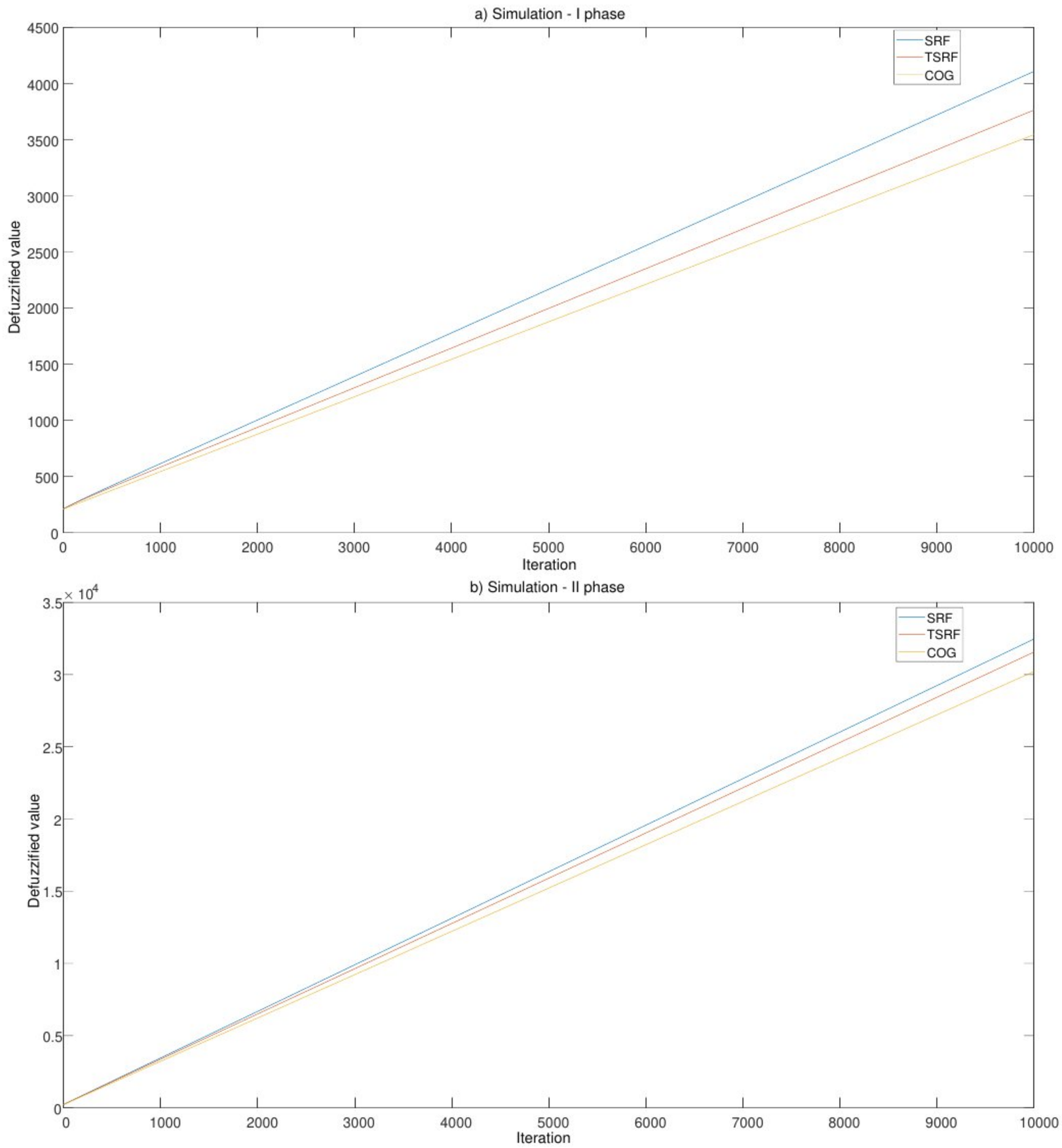

Figure 25. Comparison of defuzzification techniques TSRF, SRF and COG.

To see the deviation more clearly, the percentage deviation of the considered defuzzification techniques' results was monitored, as shown in Figure 26. As a reference value

concerning how the deviation was determined, the defuzzified values obtained by applying COG were taken.

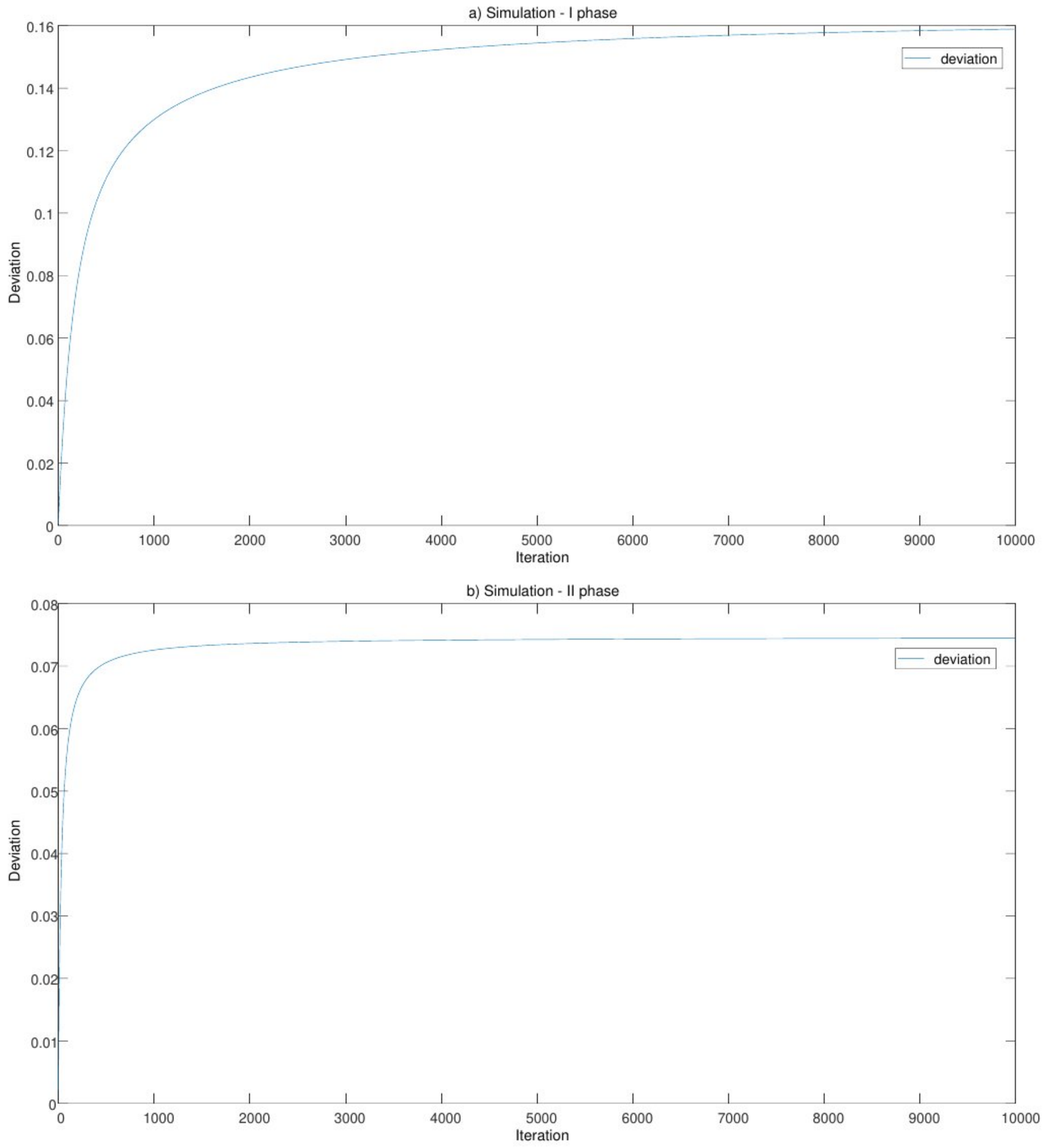

Figure 26. Deviation of TSRF and SRF results from COG.

The presented results in Figures 25 and 26 show that the TSRF and SRF provide stable results regardless of whether they are symmetric or non-symmetric fuzzy numbers.

We applied the TSRF method to transform the fuzzy objective function of the following form:

$$\begin{aligned} \min f \quad &= (16,859\ 17,576\ 20,805)x_{11,1,1} + (19,493\ 20,323\ 24,056)x_{12,1,1} + \ldots + (4762\ 5159\ 6052)x_{2019,3,3} \\ &+ (3770\ 4084\ 4791)x_{2020,3,3} + (99,880\ 112,200\ 121,000)x_1 + \ldots + (99,880\ 112,200\ 121,000)x_{20} \end{aligned} \tag{50}$$

to a crisp objective function:

$$\begin{aligned} \min f \quad &= \mathrm{TSRF}\left(\widetilde{c}\right)x_{ij,t,l} \\ &= 18,759x_{11,1,1} + 21,689x_{12,1,1} + \ldots + 5391x_{2019,3,3} + 4267x_{2020,3,3} + 11,0531x_1 + \ldots + 110,531x_{20} \end{aligned} \tag{51}$$

The pillar thickness between two operating ore passes, or the distance between candidate points, is depicted in Table 6.

Table 6. Distance between candidate points (m).

	1	**2**	**3**	**4**	**5**	**6**	**7**	**8**	**9**	**10**	**11**	**12**	**13**	**14**	**15**	**16**	**17**	**18**	**19**	**20**
1	0	10	20	30	40	50	60	70	80	90	100	110	120	130	140	150	160	170	180	190
2		0	10	20	30	40	50	60	70	80	90	100	110	120	130	140	150	160	170	180
3			0	10	20	30	40	50	60	70	80	90	100	110	120	130	140	150	160	170
4				0	10	20	30	40	50	60	70	80	90	100	110	120	130	140	150	160
5					0	10	20	30	40	50	60	70	80	90	100	110	120	130	140	150
6						0	10	20	30	40	50	60	70	80	90	100	110	120	130	140
7							0	10	20	30	40	50	60	70	80	90	100	110	120	130
8								0	10	20	30	40	50	60	70	80	90	100	110	120
9									0	10	20	30	40	50	60	70	80	90	100	110
10										0	10	20	30	40	50	60	70	80	90	100
11											0	10	20	30	40	50	60	70	80	90
12												0	10	20	30	40	50	60	70	80
13													0	10	20	30	40	50	60	70
14														0	10	20	30	40	50	60
15															0	10	20	30	40	50
16																0	10	20	30	40
17																	0	10	20	30
18																		0	10	20
19																			0	10
20																				0

According to the safety distance D = 30 m, Table 7 presents a safety matrix composed of ones and zeros. One (1) is assigned to an ore pass that does not meet the condition defined by Equation (35), otherwise zero (0).

Table 7. Safety matrix.

	1	**2**	**3**	**4**	**5**	**6**	**7**	**8**	**9**	**10**	**11**	**12**	**13**	**14**	**15**	**16**	**17**	**18**	**19**	**20**
1	0	1	1	0	0	0	0	0	0	0	0	0	0	0	0	0	0	0	0	0
2		0	1	1	0	0	0	0	0	0	0	0	0	0	0	0	0	0	0	0
3			0	1	1	0	0	0	0	0	0	0	0	0	0	0	0	0	0	0
4				0	1	1	0	0	0	0	0	0	0	0	0	0	0	0	0	0
5					0	1	1	0	0	0	0	0	0	0	0	0	0	0	0	0
6						0	1	1	0	0	0	0	0	0	0	0	0	0	0	0
7							0	1	1	0	0	0	0	0	0	0	0	0	0	0
8								0	1	1	0	0	0	0	0	0	0	0	0	0
9									0	1	1	0	0	0	0	0	0	0	0	0
10										0	1	1	0	0	0	0	0	0	0	0
11											0	1	1	0	0	0	0	0	0	0
12												0	1	1	0	0	0	0	0	0
13													0	1	1	0	0	0	0	0
14														0	1	1	0	0	0	0
15															0	1	1	0	0	0
16													0	1	1	0	0			
17														0	1	1	0			
18															0	1	1			
19																0	1			
20																	0			

The model is composed of 3620 variables and 5130 constraints, excluding binary constraints. The model is solved using Open Solver software [34]. The model selected candidate points (ore passes) x_2, x_5, x_{10}, x_{15} and x_{18} as a solution to the problem. The value of the objective function is USD 3,444,102, with an ore transportation cost component of USD 2,891,447 and an ore pass development cost component of USD 552,655. Also, the model created a unique dynamic ore transportation plan, which is depicted in Figures 27–29.

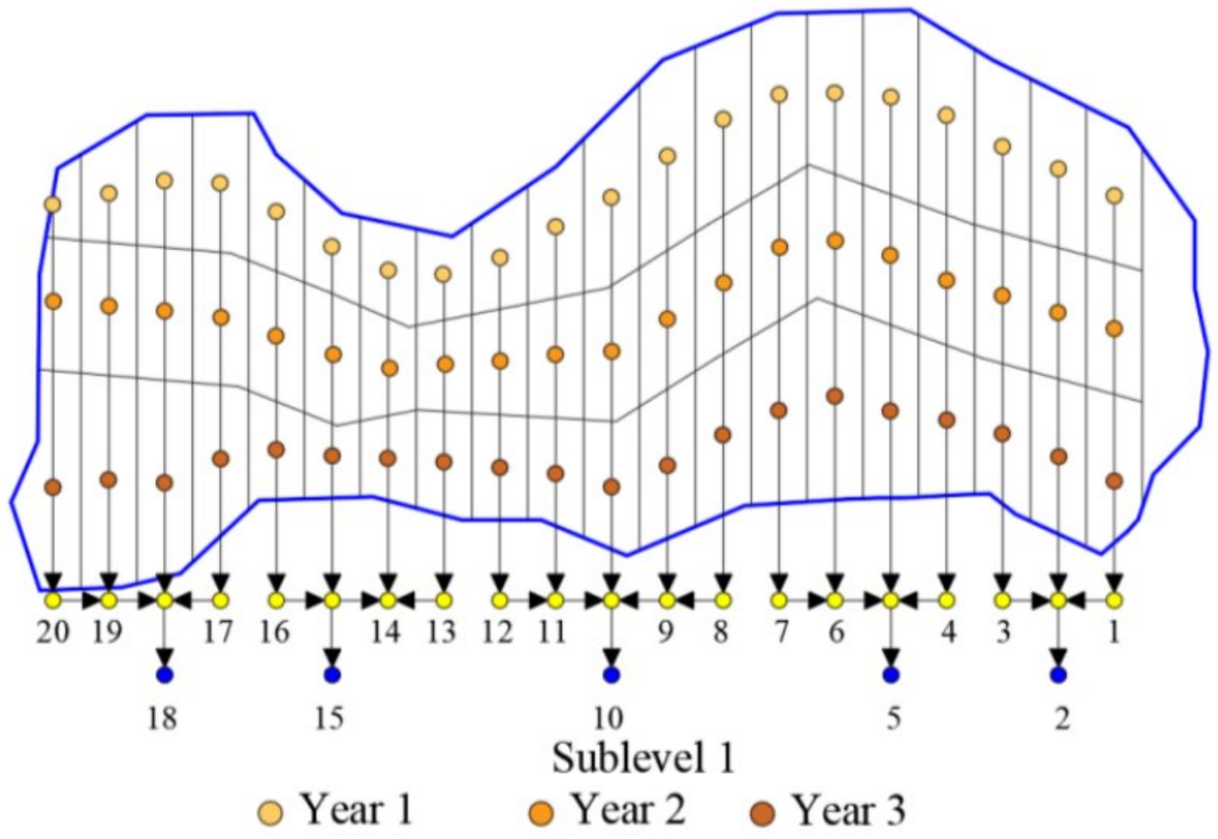

Figure 27. Ore transportation plan for $t = 1$ and $l = 1$.

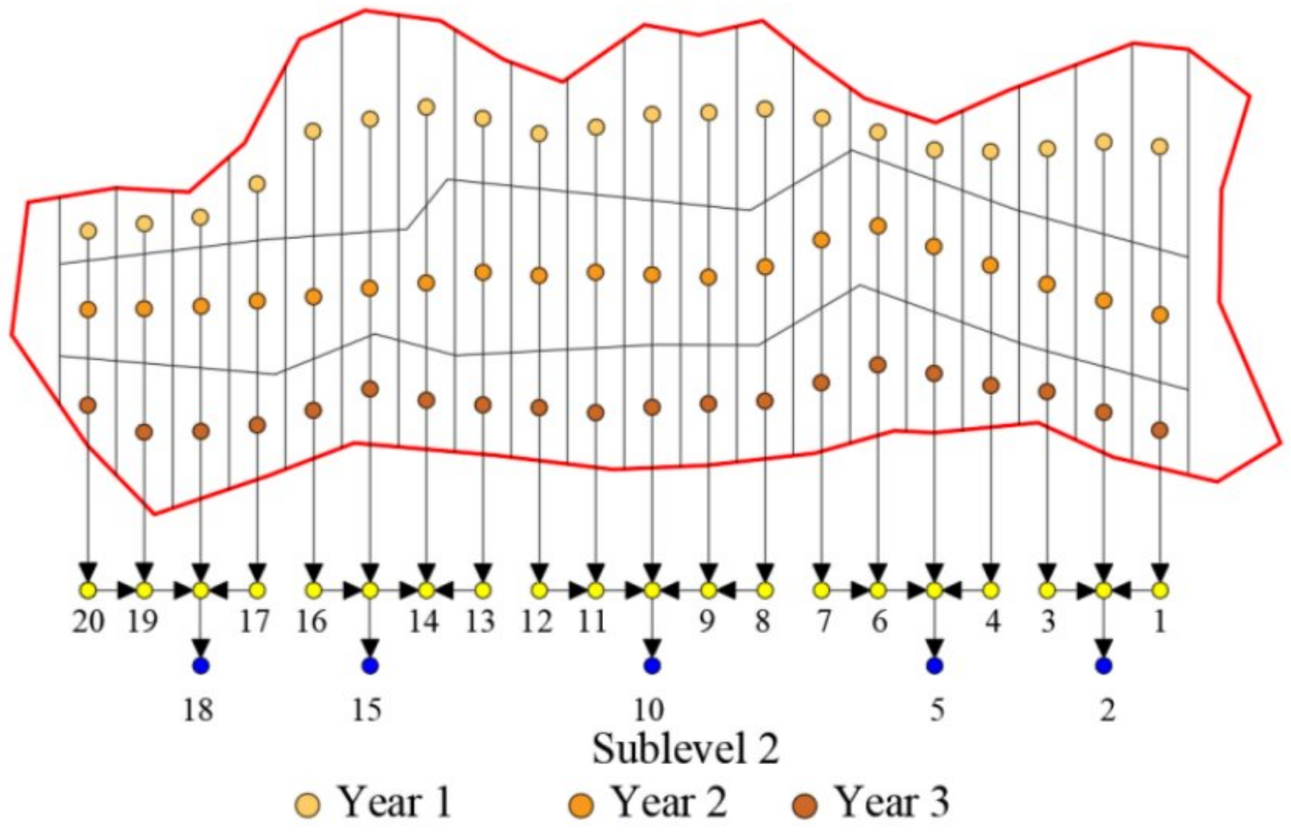

Figure 28. Ore transportation plan for $t = 2$ and $l = 2$.

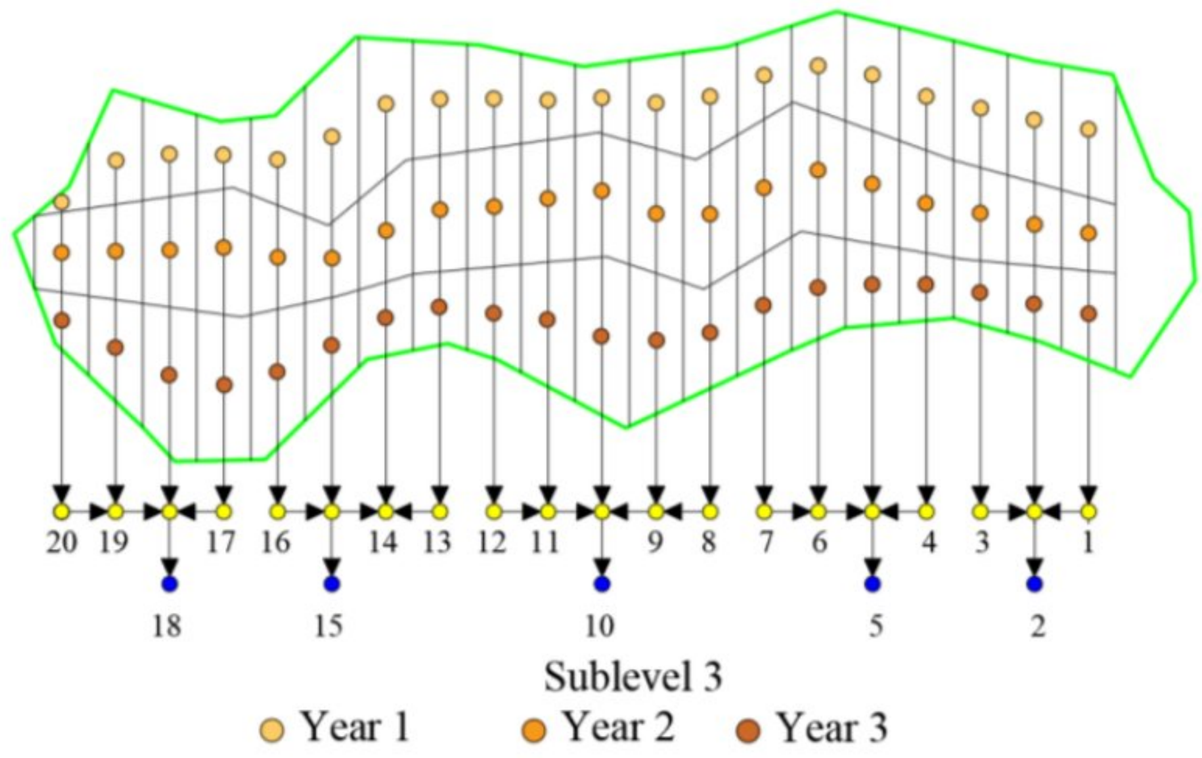

Figure 29. Ore transportation plan for $t = 3$ and $l = 3$.

The result of the dynamic ore transportation plan is explained in Table 8.

The distribution of ore tonnage by selected ore passes, for a mining period of three years, is shown in Figure 30.

The distribution of ore tonnage by selected ore passes with respect to time and sublevels is presented in Figures 31–33.

Table 8. Yearly sublevel ore transportation plan.

Year	Sublevel	Ore Pass x2 (tons)	Ore Pass x5 (tons)	Ore Pass x10 (tons)	Ore Pass x15 (tons)	Ore Pass x18 (tons)
1	1	18,563	27,865	31,283	15,860	16,735
	2	20,789	12,839	30,449	29,336	12,839
	3	15,185	16,775	18,365	20,829	11,766
2	1	15,741	21,227	25,440	17,888	19,756
	2	15,741	21,306	29,216	21,505	18,166
	3	10,256	19,557	25,679	16,735	16,934
3	1	17,649	28,024	26,195	14,549	30,409
	2	9858	19,796	23,413	16,139	18,126
	3	9421	14,986	25,639	15,781	18,245

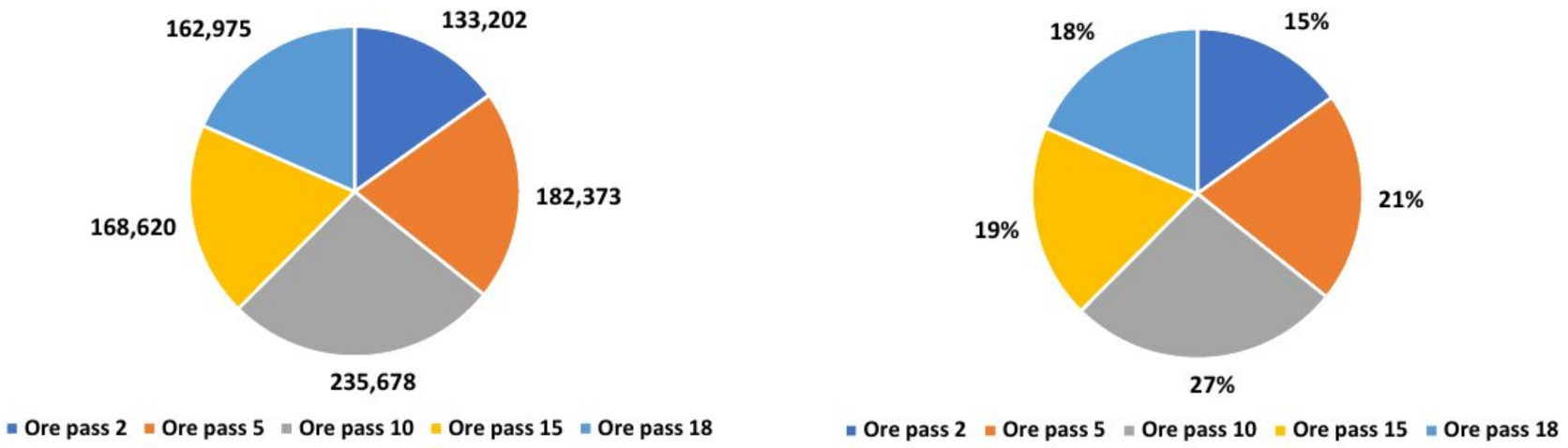

Figure 30. The distribution of ore tonnage by selected ore passes.

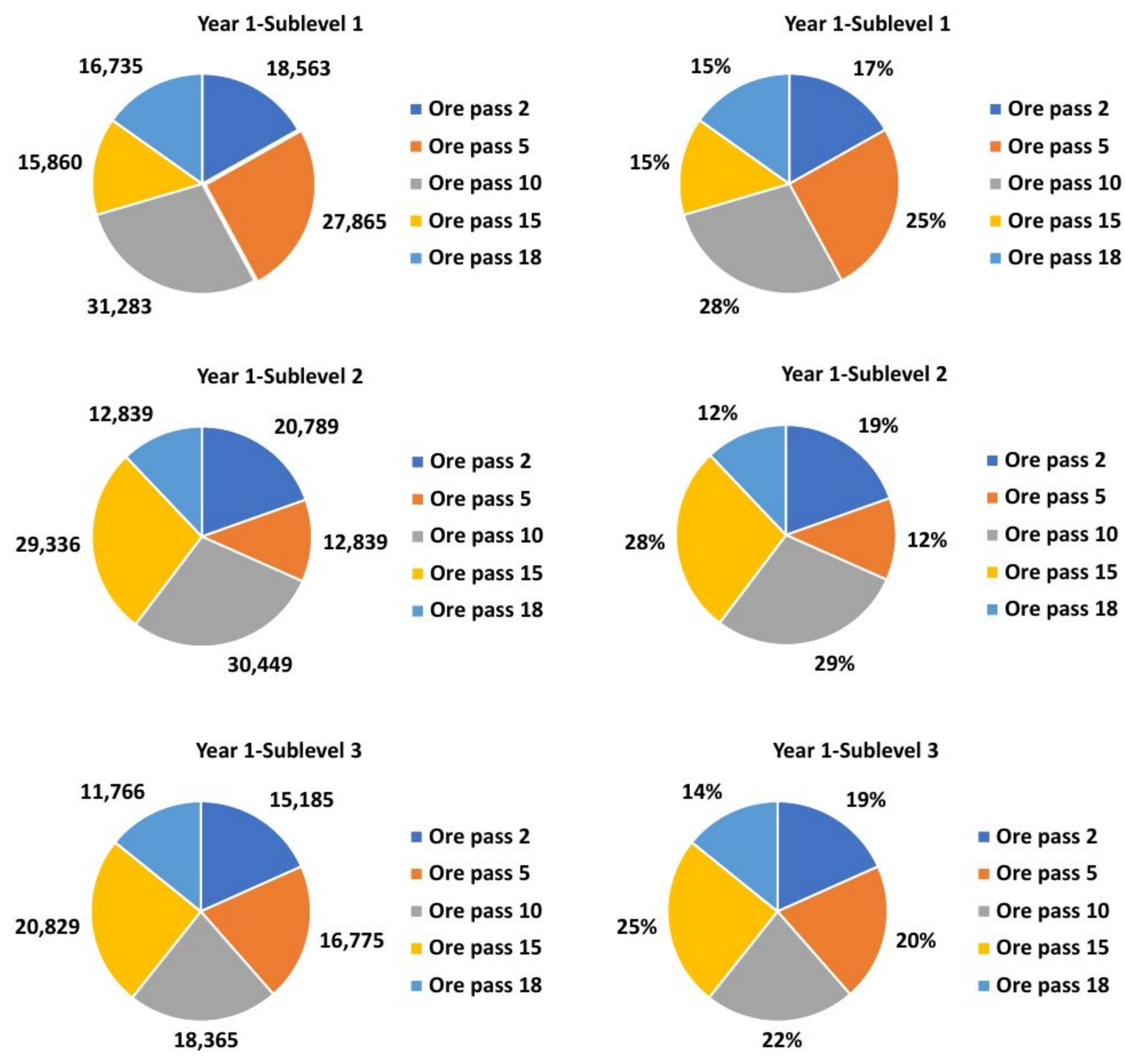

Figure 31. The distribution of ore tonnage by ore passes through sublevels for year 1.

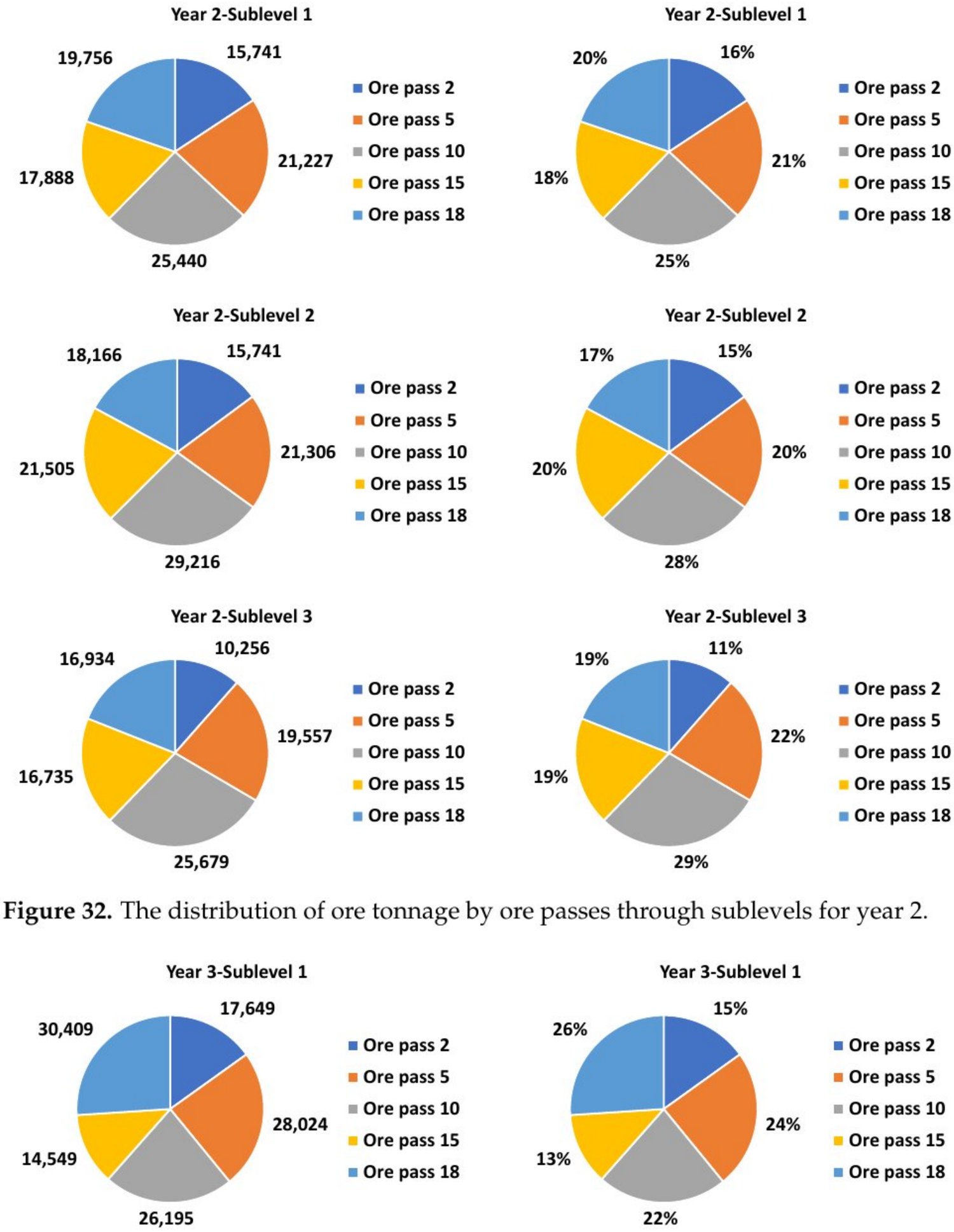

Figure 32. The distribution of ore tonnage by ore passes through sublevels for year 2.

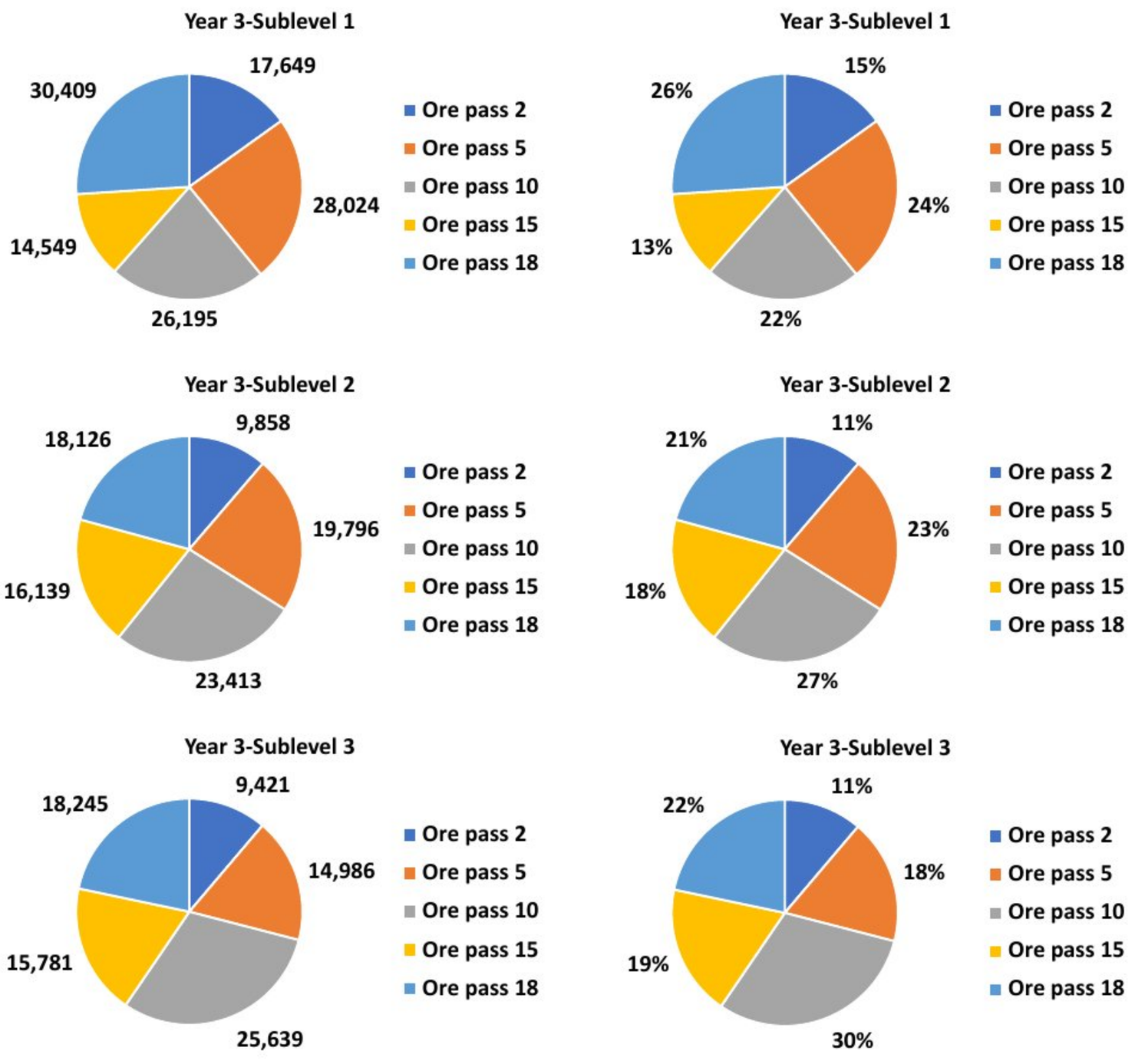

Figure 33. The distribution of ore tonnage by ore passes through sublevels for year 3.

As we mentioned above, total transportation costs are USD 2,891,447, and the time distribution of costs is depicted in Figure 34.

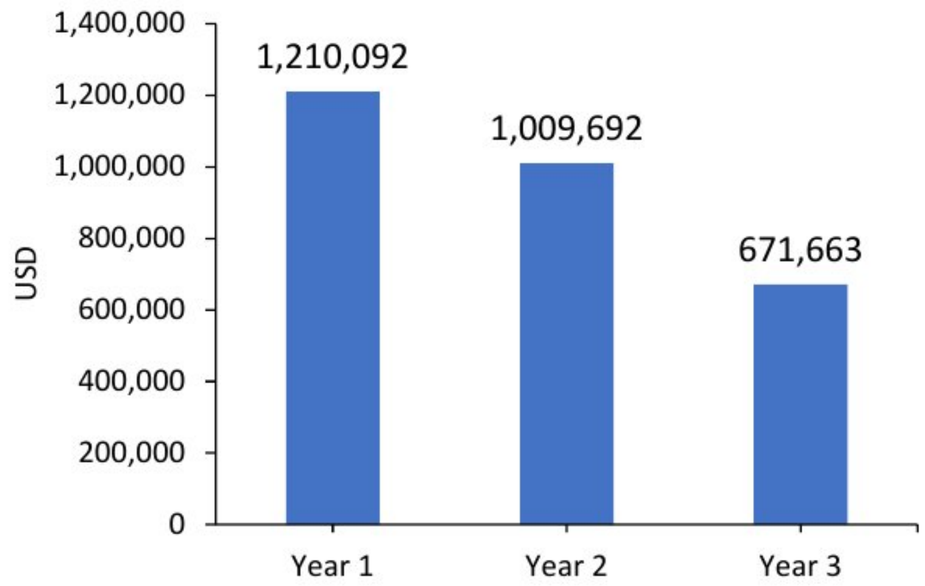

Figure 34. Transportation costs on yearly time resolution.

5. Sensitivity Analysis of the Model

The model produced a solution with following properties:

- Selected ore passes are x_2, x_5, x_{10}, x_{15} and x_{18};
- Value of objective function is USD 3,444,102;
- Value of ore transportation costs is USD 2,891,447;
- Value of ore pass development costs is USD 552,655;
- Ratio between transportation and development costs is 5.23.

Obviously, the component of the objective function relating to the ore transportation costs has the greatest influence on the solution, followed by the ore pass development costs. So, the sensitivity analysis is based on changes in the coefficients of the objective function, which present the unit transportation costs (see Table 9).

Table 9. Magnitude of changes in unit transportation costs.

Magnitude of Change (%)	Unit Transportation Cost Year 1, (USD/tm)			Unit Transportation Cost Year 2, (USD/tm)			Unit Transportation Cost Year 3, (USD/tm)		
−50	0.024	0.025	0.029	0.026	0.029	0.031	0.024	0.026	0.031
−45	0.026	0.027	0.032	0.028	0.031	0.034	0.026	0.029	0.034
−40	0.028	0.029	0.035	0.031	0.034	0.037	0.029	0.031	0.037
−35	0.031	0.032	0.038	0.033	0.037	0.040	0.031	0.034	0.040
−30	0.033	0.034	0.041	0.036	0.040	0.043	0.034	0.036	0.043
−25	0.035	0.037	0.044	0.038	0.043	0.047	0.036	0.039	0.046
−20	0.038	0.039	0.046	0.041	0.046	0.050	0.038	0.042	0.049
−15	0.040	0.042	0.049	0.043	0.048	0.053	0.041	0.044	0.052
−10	0.042	0.044	0.052	0.046	0.051	0.056	0.043	0.047	0.055
−5	0.045	0.047	0.055	0.048	0.054	0.059	0.046	0.049	0.058
0	0.047	0.049	0.058	0.051	0.057	0.062	0.048	0.052	0.061
5	0.049	0.051	0.061	0.054	0.060	0.065	0.050	0.055	0.064
10	0.052	0.054	0.064	0.056	0.063	0.068	0.053	0.057	0.067
15	0.054	0.056	0.067	0.059	0.066	0.071	0.055	0.060	0.070
20	0.056	0.059	0.070	0.061	0.068	0.074	0.058	0.062	0.073
25	0.059	0.061	0.073	0.064	0.071	0.078	0.060	0.065	0.076
30	0.061	0.064	0.075	0.066	0.074	0.081	0.062	0.068	0.079
35	0.063	0.066	0.078	0.069	0.077	0.084	0.065	0.070	0.082
40	0.066	0.069	0.081	0.071	0.080	0.087	0.067	0.073	0.085
45	0.068	0.071	0.084	0.074	0.083	0.090	0.070	0.075	0.088
50	0.071	0.074	0.087	0.077	0.086	0.093	0.072	0.078	0.092

For each change in fuzzy unit transportation costs, we ran the model, and the results of the changes are shown in Table 10 and Figure 35.

Table 10. Results of the sensitivity analysis.

Magnitude of Change (%)	Total Costs (USD)	Transportation Costs (USD)	Development Costs (USD)	Total Number of Ore Passes
−50	1,931,604	1,600,011	331,593	3
−45	2,087,657	1,645,533	442,124	4
−40	2,237,250	1,795,126	442,124	4
−35	2,386,844	1,944,720	442,124	4
−30	2,536,438	2,094,314	442,124	4
−25	2,686,032	2,243,908	442,124	4
−20	2,835,626	2,393,502	442,124	4
−15	2,985,220	2,543,096	442,124	4
−10	3,134,814	2,692,690	442,124	4
−5	3,284,407	2,842,283	442,124	4
0	3,444,102	2,891,447	552,655	5
5	3,589,021	3,036,366	552,655	5
10	3,736,805	3,184,150	552,655	5
15	3,868,816	3,316,161	552,655	5
20	4,020,593	3,357,407	552,655	5
25	4,161,238	3,608,583	552,655	5
30	4,297,119	3,633,933	663,186	5
35	4,431,073	3,767,887	663,186	6
40	4,570,624	3,907,438	663,186	6
45	4,710,175	4,046,989	663,186	6
50	4,849,727	4,186,541	663,186	6

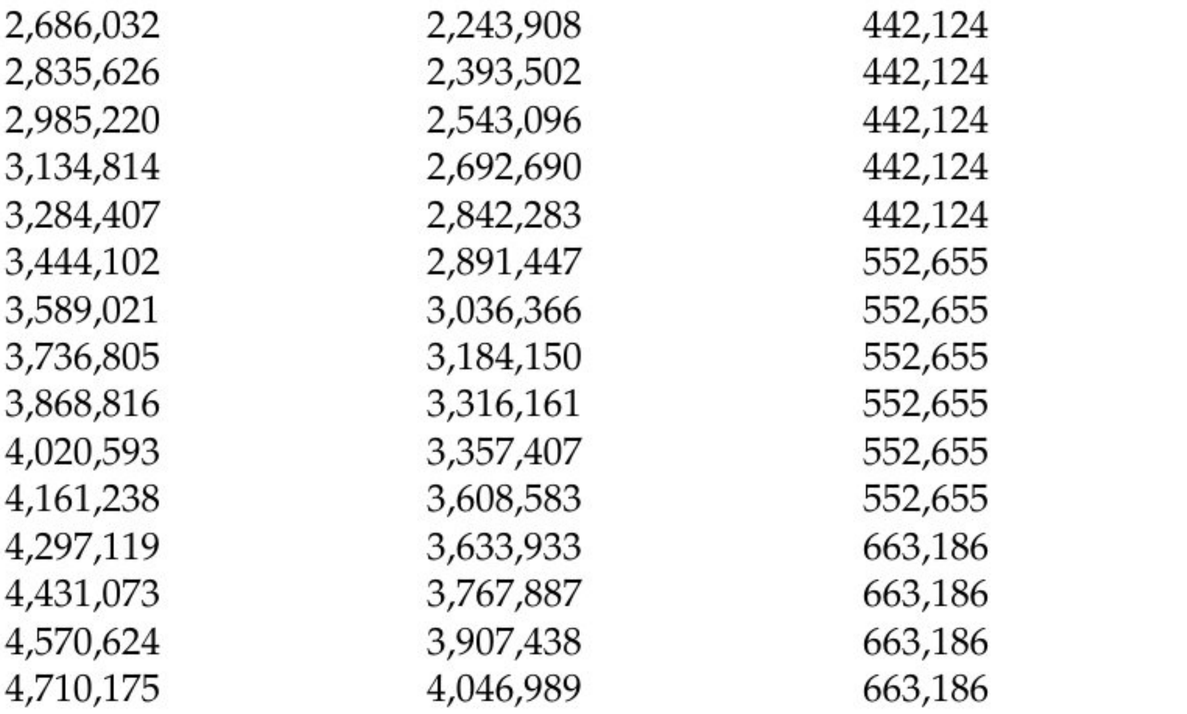

Figure 35. Number of ore passes vs. costs.

The results of the sensitivity analysis show the model is stable, and underground mine designers can use it for solving this complex problem.

6. Conclusions

This paper has demonstrated that an integrated planning tool can provide an especially useful support for obtaining the globally optimal result, by considering interaction between ore transportation and ore pass design costs, with uncertainty. Fuzzy triangular numbers are used to quantify the uncertainties of objective function coefficients. To reduce the complexity of the optimization model with uncertainty, we developed a methodology which transforms the fuzzy 0-1 linear cost objective function of ore passes into a crisp one. This transformation is based on the application of Graph theory and the algorithm of the Torricelli point, which lies at the intersection of the Simpson lines. The x-coordinate of the Torricelli point is a crisp value of a triangular fuzzy number. We performed a comparison with some of the existing methods and a stability analysis of the proposed methodology, which showed that the Torricelli–Simpson method is very capable of transforming a fuzzy

environment into a crisp environment. In the Appendix A section, we showed additional benefits of the developed model, which relate to the ranking of special cases of triangular fuzzy numbers.

In essence, the ore passes optimization problem is a location–allocation problem but with an added space–time component, according to the nature of sublevel mining methods. From the finite set of potential ore pass locations, the model selects the optimal number and optimal locations of ore passes, by minimizing the total costs of ore transportation and ore pass development with respect to techno-dynamic constraints. In addition, the model also creates an optimal ore transportation plan. The sensitivity analysis, which considered the changes in ore transportation costs, showed that model is capable of discovering an equilibrium between them and the total number of ore passes. The main aim of the model is to help mine designers to solve such complex problems, which have a significant influence on mining economics.

The proposed fuzzy linear programming model extends linear programming to handle fuzzy constraints and objectives, but it has certain limitations that should be considered. These limitations derive from the basic limitations of fuzzy linear models:

- The proposed methodology can introduce additional complexity compared to traditional linear programming due to the incorporation of fuzzy variables, fuzzy constraints, and fuzzy objectives.
- Solving the proposed fuzzy linear programming model can be computationally demanding, especially for large-scale or complex optimization models.
- In the case of expanding the proposed model by introducing subjective linguistic assessments, it can lead to inconsistent or subjective results. This limitation comes from the subjective nature of the membership functions and linguistic terms used to represent uncertainty in expert judgments.

Despite these limitations, the proposed fuzzy linear model remains a valuable tool for decision-making under uncertainty. By carefully considering its limitations and choosing appropriate methodologies, the proposed fuzzy linear model can provide insights into and solutions to real-world problems.

In this study, a novel approach for the defuzzification of TFNs using the Torricelli–Simpson ranking function (TSRF) is proposed. Since the proposed model showed stable results, future research should be directed toward the implementation of the TSRF for the defuzzification of trapezoidal fuzzy numbers. Also, an interesting direction of future research is the consideration of the possibility of applying the TSRF for reading the footprint of uncertainty in information and transforming TFNs into interval type-2 fuzzy numbers. In addition to the mentioned directions of future research, there are also possibilities of applying the TSRF for the transformation of interval type-2 fuzzy numbers into crisp values. Also, further research will be directed toward developing an integrated model which will join the planning of mining and the planning of ore passes. Such a model must be capable of giving the optimal solution for mining planning and ore passes planning simultaneously. Accordingly, it is necessary to develop a specific cash flow objective function which should be maximized with respect to a set of constraints.

Author Contributions: Conceptualization, D.H. and Z.G.; methodology, D.H. and Z.G.; validation, M.G. and D.P.; formal analysis, D.H. and D.P.; investigation, M.G. and Z.G.; data curation, D.H., M.G. and D.P.; writing—original draft preparation, D.H. and Z.G.; writing—review and editing, M.G. and Z.G.; visualization, D.H. and D.P.; supervision, Z.G. All authors have read and agreed to the published version of the manuscript.

Funding: This research received no external funding.

Data Availability Statement: Not applicable.

Conflicts of Interest: The authors declare no conflict of interest.

Appendix A

Recall the definition of triangular fuzzy number.

Definition A1. *Let X be a universe set. A fuzzy set A of X is defined by a following membership function* $\mu_A(x) \to [0,1]$, *where* $\mu_A(x), \forall x \in X$, *indicates the degree of x in A.*

Definition A2. *A fuzzy subset A of universe set X is normal if and only if* $\sup_{x \in X} \mu_A(x) = 1$, *where* X *is the universe set.*

Definition A3. *A fuzzy subset A of universe set X is convex if and only if* $\mu_A(\beta x + (1-\beta)y) \geq \min(\mu_A(x), \mu_A(y)), \forall x, y \in X, \forall \beta \in [0,1]$.

Definition A4. *A fuzzy set A is a triangular fuzzy number if and only if A is normal and convex on X.*

Accordingly, properties of a triangular fuzzy number are as follows:

- $\mu(x)$ is upper semicontinuous;
- There are real numbers a, b, c; $a \leq b \leq c$, for which the following holds: $\mu(x)$ is monotonic increasing function on [a,b], monotonic decreasing function on [b,c] and $\mu(x) = 1$ for x = b;
- $\mu(x) = 0$, outside interval [a,c].

A symmetric triangular fuzzy number is defined as:

$$\mu_{\tilde{A}}(x) = \begin{cases} 0, & x \leq a \\ \frac{x-a}{b-a}, & a \leq x \leq b \\ \frac{c-x}{c-b}, & b \leq x \leq c \\ 0, & x \geq c \\ b-a = c-b \end{cases}, \tag{A1}$$

To present the additional benefit of the TSRF, we borrowed an example from Saneifard [35]. Consider the two symmetric triangular fuzzy numbers, $A(1,3,5)$ and $B(2,3,4)$, which are shown in Figure A1. Numbers A and B have equal modes but different spreads.

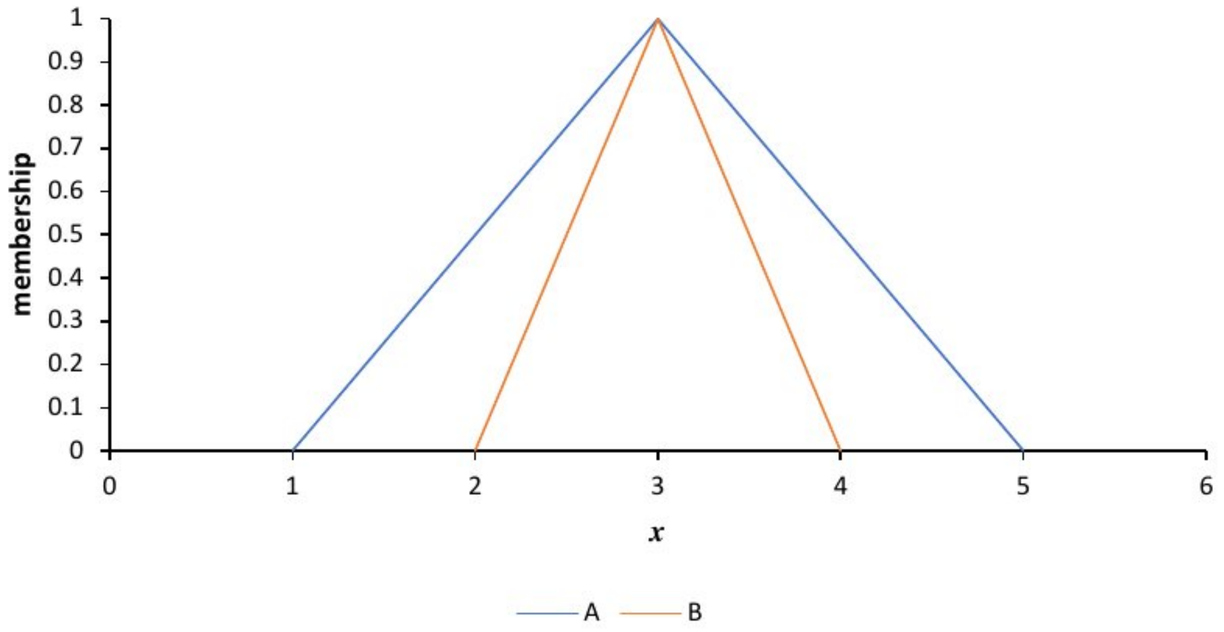

Figure A1. Two symmetric triangular fuzzy numbers with equal modes.

Let Δx be a small increment close to zero. By adding up Δx to the mode of numbers A and B, respectively, we create prerequisites to apply the TSRF for ranking two symmetric triangular fuzzy numbers, without a loss of generality. For $\Delta x = 0.001$, we obtain $A(1,3.001,5)$, $B(2,3.001,4)$ and the corresponding TSRF(A) = 3.000267, TSRF(B) = 3.000161. So, the following ranking order of fuzzy numbers is $A > B$. The ranking index values obtained by Saneifard's approach are I(A) = 2.5, I(B) = 2, and the ranking order of fuzzy numbers is $A > B$. The center of gravity of A and B equals COG(A) = COG(B) = 3.000333

and ranking order is $A = B$. Obviously, the TSRF is capable of ranking symmetric triangular fuzzy numbers with equal modes and different spreads.

The TSRF algorithm is also capable of ranking the symmetric triangular fuzzy numbers with equal modes but with different membership functions. If A and B are two triangular fuzzy numbers, then the following rules are used to rank such kinds of triangular fuzzy numbers:

$$\begin{cases} A > B, & \text{if } \mathrm{TSRF}(A) > \mathrm{TSRF}(B), \\ A > B, & \text{if } \mathrm{TSRF}(A) < \mathrm{TSRF}(B), \text{for } b - a > c - b, \\ A > B, & \text{if } \mathrm{TSRF}(A) < \mathrm{TSRF}(B), \text{for } b - a > c - b \wedge a + b + c < 0. \end{cases} \tag{A2}$$

This ability is demonstrated by the following special case. Consider two triangular fuzzy numbers $A = (0.1, 0.3, 0.5, \mu(0.3) = 0.8)$ and $B = (0.1, 0.3, 0.5, \mu(0.3) = 1)$ [36] (see Figure A2).

Figure A2. Two symmetric triangular fuzzy numbers with equal modes and different membership functions.

For $\Delta x = 0.001$, we obtain $A = (0.1, 0.301, 0.5, \mu(0.301) = 0.8)$, $B = (0.1, 0.301, 0.5, \mu(0.301) = 1)$ and the corresponding TSRF(A) = 0.300267, TSRF(B) = 0.300286. For number A and number B, $b - a = 0.201$, and $c - b = 0.199$. According to Equation (A2), it follows that $A < B$. A new parametric method developed by Shureshjani and Darehmiraki ranks fuzzy numbers A and B in the same way.

References

1. Maree, J.A. Orepass best practices at South Deep. *J. South. Afr. Inst. Min. Metall.* **2011**, *111*, 257–272.
2. Hadjigeorgiou, J.; Stacey, T.R. The absence of strategy in orepass planning, design, and management. *J. South. Afr. Inst. Min. Metall.* **2013**, *113*, 795–801.
3. Skawina, B.; Greberg, J.; Salama, A.; Gustafson, A. The effects of orepass loss on loading, hauling, and dumping operations and production rates in a sublevel caving mine. *J. South. Afr. Inst. Min. Metall.* **2018**, *118*, 409–418. [CrossRef]
4. Sredniawa, W.; Skawina, B.; Rapp, J.; Shekhar, G.; Gunillasson, J. Longevity chart for planning production and the renovation of orepasses. In Proceedings of the Caving 2022: Fifth International Conference on Block and Sublevel Caving, Perth, Australia, 30 August–1 September 2022; Potvin, Y., Ed.; Australian Centre for Geomechanics: Perth, Australia, 2022; pp. 369–380. [CrossRef]
5. Adjiski, V.; Panov, Z.; Popovski, R.; Karanakova Stefanovska, R. Implementation of discrete element method to evaluate the design and material flow in ore pass systems. In Proceedings of the Seventh National Scientific and Technical Conference with International Participation: Technologies and Practices in Underground Mining and Mine Construction, Devin, Bulgaria, 5–8 October 2020; pp. 37–46.
6. Hadjigeorgiou, J.; Esmaieli, K.; Harrisson, R. Observation of ore pass system performance at Brunswick Mine. *CIM Bull.* **2008**, *101*, 1110.
7. Chen, H.; Yu, S.; Wang, Z.; Yuan, Y. A New Plugging Technology and Its Application for the Extensively Collapsed Ore Pass in the Non-Empty Condition. *Energies* **2018**, *11*, 1599. [CrossRef]
8. Esmaieli, K.; Hadjigeorgiou, J.; Grenon, M. Stability analysis of the 19A ore pass at Brunswick mine using a two-stage numerical modeling approach. *Rock Mech. Rock Eng.* **2013**, *46*, 1323–1338. [CrossRef]

9. Gardner, L.J.; Fernandes, N.D. Ore pass rehabilitation–case studies from impala platinum limited. *J. South. Afr. Inst. Min. Metall.* **2006**, *106*, 17–23.
10. Greberg, J.; Salama, A.; Gustafson, A.; Skawina, B. Alternative Process Flow for Underground Mining Operations: Analysis of Conceptual Transport Methods Using Discrete Event Simulation. *Minerals* **2016**, *6*, 65. [CrossRef]
11. Li, N.; Feng, S.; Lei, T.; Ye, H.; Wang, Q.; Wang, L.; Jia, M. Rescheduling Plan Optimization of Underground Mine Haulage Equipment Based on Random Breakdown Simulation. *Sustainability* **2022**, *14*, 3448. [CrossRef]
12. Hou, J.; Li, G.; Chen, L.; Wang, H.; Hu, N. Optimization of Truck–Loader Matching Based on a Simulation Method for Underground Mines. *Sustainability* **2023**, *15*, 216. [CrossRef]
13. Koivisto, M. Ore Pass Design and Placement. Master's Thesis, Delft University of Technology, Delft, The Netherlands, 30 August 2017.
14. Zadeh, L.A. *Fuzzy Sets, Fuzzy Logic and Fuzzy Systems*; World Scientific: Singapore, 1996.
15. Yager, R.R. Ranking Fuzzy Subsets over the Unit Interval. In Proceedings of the 1978 IEEE Conference on Decision and Control Including the 17th Symposium on Adaptive Processes, San Diego, CA, USA, 10–12 January 1979; pp. 1435–1437.
16. Chen, S.H. Ranking fuzzy numbers with maximizing set and minimizing set. *Fuzzy Sets Syst.* **1985**, *17*, 113–129. [CrossRef]
17. Liou, T.S.; Wang, M.J. Ranking fuzzy numbers with integral value. *Fuzzy Sets Syst.* **1992**, *50*, 247–256. [CrossRef]
18. Adamo, J. Fuzzy decision trees. *Fuzzy Sets Syst.* **1980**, *4*, 207–219. [CrossRef]
19. González, A. A study of the ranking function approach through mean values. *Fuzzy Sets Syst.* **1990**, *35*, 29–41. [CrossRef]
20. Chutia, R. A Novel Defuzzification Approach of Ranking Parametric Fuzzy Numbers Based on the Value and Ambiguity Calculated at Decision Levels. *Int. J. Uncertain. Fuzziness Knowl.-Based Syst.* **2022**, *30*, 847–878.
21. Dutta, P. A sophisticated ranking method of fuzzy numbers based on the concept of exponential area. *New Math. Nat. Comput.* **2021**, *17*, 303–318.
22. Zou, S.C.; Liu, F.; You, Q.R. A Two-Dimensional Simulation Approach for Ranking Fuzzy Numbers by the Monte Carlo Technique. *Int. J. Uncertain. Fuzziness Knowl.-Based Syst.* **2021**, *29*, 559–586. [CrossRef]
23. Wang, Z.X.; Mo, Y.N. Ranking fuzzy numbers based on ideal solution. In *Fuzzy Information and Engineering: Advances in Soft Computing*; Cao, B.Y., Zhang, C.Y., Li, T.F., Eds.; Springer: Berlin, Germany, 2009; Volume 54, pp. 201–209.
24. Pourabdollah, A.; Mendel, J.M.; John, R.I. Alpha-cut representation used for defuzzification in rule-based systems. *Fuzzy Sets Syst.* **2020**, *399*, 110–132. [CrossRef]
25. Asady, B.; Zendehnam, A. Ranking Fuzzy Numbers by Distance Minimization. *Appl. Math. Model.* **2007**, *31*, 2589–2598. [CrossRef]
26. Brazil, M.; Graham, R.L.; Thomas, D.A.; Zachariasen, M. On the history of the Euclidean Steiner tree problem. *Arch. Hist. Exact Sci.* **2014**, *68*, 327–354.
27. Darling, P. *SME Mining Engineering Handbook*; SME: Englewood, CO, USA, 2011.
28. Cokayne, E.W. Sublevel Caving Chapter 1: Introduction. In *Underground Mining Methods Handbook*; Hustrulid, W.A., Ed.; Society of Mining Engineers of the American Institute of Mining, Metallurgical and Petroleum Engineers: New York, NY, USA, 1982.
29. Hustrulid, W.A.; Bullock, R.C. *Underground Mining Methods: Engineering Fundamentals and International Case Studies*; Society for Mining, Metallurgy, and Exploration: Littleton, CO, USA, 2001.
30. Laubscher, D.H. Cave mining-the state of the art. *J. South. Afr. Inst. Min. Metall.* **1994**, *94*, 279–293.
31. Available online: https://www.engineerlive.com/sites/engineerlive/files/SCHOPF-SFL60XLP-FLP_0.jpg (accessed on 14 January 2023).
32. Bunker, K.; Campbell, A.; O'Toole, D.; Penney, A. Guidelines for orepass design in a sublevel cave mine. In Proceedings of the International Seminar on Design Methods in Underground Mining, Perth, Australia, 17–19 November 2015; Potvin, Y., Ed.; Australian Centre for Geomechanics: Perth, Australia, 2015.
33. Garrido, B.P.; Sebrek, S.S.; Semenova, V. Comparing different ranking functions for solving fuzzy linear programming problems with fuzzy cost coefficients. *Hung. Stat. Rev.* **2021**, *4*, 3–17. [CrossRef]
34. Mason, A.J. OpenSolver—An Open Source Add-in to Solve Linear and Integer Progammes in Excel. In *Operations Research Proceedings 2011*; Klatte, D., Lüthi, H.J., Schmedders, K., Eds.; Springer: Berlin/Heidelberg, Germany, 2012; pp. 401–406; ISBN 978-3-642-29209-5.
35. Saneeifard, R. Ranking LR fuzzy numbers with weighted averaging based on levels. *Int. J. Ind. Math.* **2009**, *1*, 163–173.
36. Shureshjani, R.A.; Darehmiraki, M. A new parametric method for ranking fuzzy numbers. *Indag. Math.* **2013**, *24*, 518–529. [CrossRef]